Pre-Clinical Evaluation of Biopolymer Delivered Circulating Angiogenic Cells in Hibernating Myocardium

Céline Giordano

This thesis is submitted as a partial fulfilment of the M.Sc. program in the department of Cellular and Molecular Medicine

uOttawa

Department of Cellular and Molecular Medicine

Faculty of Medicine

University of Ottawa

Division of Cardiac Surgery

University of Ottawa Heart Institute

ABSTRACT

Vasculogenic cell-based therapy combined with tissue engineering is a promising revascularization strategy for patients with hibernating myocardium, a common clinical condition. We used a clinically relevant swine model of hibernating myocardium to examine the benefits of biopolymer-supported delivery of circulating angiogenic cells (CACs) in this context.

Twenty-five swine underwent placement of an ameroid constrictor on the left circumflex artery (LCx). After 2 weeks, positron emission tomography measures of myocardial blood flow (MBF) and myocardial flow reserve (MFR) were reduced in the affected region (both $p<0.001$). Hibernation (mismatch) was specific to the LCx territory. Swine were randomized to receive intramyocardial injections of PBS control (n=10), CACs (n=8), or CACs + a collagen-based matrix (n=7). At follow-up, stress MBF and MFR were increased only in the cells+matrix group ($p<0.01$), and mismatch was lower in the cells+matrix treated animals ($p=0.02$) compared to controls. Similar results were found using microsphere-measured MBF. Wall motion abnormalities and ejection fraction improved only in the cells+matrix group.

This preclinical swine model demonstrated ischemia and hibernation, which was improved by the combined delivery of CACs and a collagen-based matrix. To our knowledge, this is the first demonstration of the mechanisms and effects of combining progenitor cells and biopolymers in the setting of myocardial hibernation, a common clinical condition in patients with advanced coronary artery disease.

TABLE OF CONTENTS

LIST OF FIGURES

LIST OF TABLES

LIST OF ABBREVIATIONS

Acronym	Definition
AC	= Attenuation correction
Ang	= Angiopoietin
BM	= Bone marrow
CABG	= Coronary artery bypass grafting
CAC	= Circulating angiogenic cell
CAD	= Coronary artery disease
CPC	= Circulating progenitor cell
CSC	= Cardiac stem cell
CT	= Computed tomography
CTA	= Computed tomography angiography
DSE	= Dobutamine stress echocardiography
EBM	= Endothelial basal media
EC	= Endothelial cell
ECFC	= Endothelial colony forming cell
ECM	= Extra- cellular matrix
EGM	= Endothelial growth media
eNOS	= Endothelial nitric oxide synthase
EPC	= Endothelial progenitor cell
FBS	= Foetal bovine serum
FDG	= Fluorodeoxyglucose
FGF	= Fibroblast growth factor
FS	= Fractional shortening
HIF	= Hypoxia-inducible factor
H&E	= Haematoxylin and eosin
ILM	= Isotope labelled microspheres

iPS = Induced pluripotent stem (cell)

LAD = Left anterior descending (coronary artery)

LCx = Left circumflex (coronary artery)

LDL = Low density lipoprotein

LV = Left ventricle

LVEF = Left ventricular ejection fraction

MBF = Myocardial blood flow

MBq = Mega Becquerel

MFR = Myocardial flow reserve

MCE = Myocardial contrast enhanced echocardiography

MSC = Mesenchymal stem cell

MNC = Mononuclear cell

MRI = Magnetic resonance imaging

NH_3 = Ammonia

NO = Nitric oxide

PECAM = Platelet endothelial cell adhesion molecule

PET = Positron emission tomography

PB = Peripheral blood

PBS = Phosphate buffered saline

SDF-1 = Stromal derived factor -1

SMA = Smooth muscle actin

SPECT = Single photon emission computed tomography

TIMI = Thrombolysis in myocardial infarction

VE-cadherin = Vascular endothelial-cadherin

VEGF = Vascular endothelial growth factor

VEGF-R2 = Vascular endothelial growth factor receptor 2

vWF = von Willebrand factor

WMSI = Wall motion score index

ACKNOWLEDGEMENTS

First and foremost, I would like to sincerely thank my supervisor Dr. Marc Ruel for his great mentorship, his eternal positivism and his sense of humour. I would like to thank him for presenting me with a project I fully enjoyed, and for always putting a smile on my face, even when I arrived discouraged in his office. I am very grateful for his support and encouragements, for his insightful suggestions, and for the invaluable learning experience he offered me.

I would also like to thank my co-supervisor Dr. Erik Suuronen for his guidance and availability that were always very helpful. In addition, I would like to extend my gratitude to my committee members, Dr. Rob Beanlands and Dr. Rob deKemp for their enthusiasm and direction during my Master's.

I would like to acknowledge the tremendous help I received from Stephanie Thorn. From the first day, she was always available to answer my questions, to guide me through my experiments and to help me solve many problems. This project would not have been possible without her contribution. I also thank her for the many nights she stayed late scanning my animals, while learning about Swiss culture and rock-climbing.

I would like to thank Jennifer Renaud for her expertise in image analysis; she was dedicated and patient in teaching me how to analyse scans, and in helping me troubleshoot problems I encountered. Thank you to Ran Klein for working on any request I had, and for making my shuttle bus rides to work more enjoyable. Thank you to Julia Lockwood for her help in CT image acquisition and for being the best french student I ever had. Thank you to Dr. Glenn Wells for lending me his program to generate

microsphere polar maps, and to Dr. Corinne Bensimon for teaching me how to use it. Thank you to Richard Tessier for instructing me in acquiring CT angios, and to May Aung and Kim Gardner for their assistance during imaging sessions and their help for scan reconstructions.

I would like also to thank all my lab colleagues in the Regenerative Therapy and Tissue Engineering Laboratories. During the past two years, I had the chance to meet a variety of people who made my time at the Heart Institute an enjoyable one. Thank you to Donna Padavan, Chenchen Hou, Mary Zhang, Branka Vulesevic, Jenelle Marier, Tanja Sofrenovic, Joanne McBane and Ali Ahmadi. Of course a special thank to Drew Kuraitis for his availability and his advises, even after his departure to Rome.

I would also like to extend my gratitude to the Animal Care staff; they were always dedicated to take excellent care of my animals and provide assistance for scans and surgeries. A special thanks to Dan de Vette for his surgical skills and to Dr. Talal AlAtassi for his work in surgery, as well as his unconscious efforts to help me discover the marvellous world of medical residents.

A special thanks to Suzanne Crowe for her efforts to bring this project to an end.

Thank you to the Heart and Stroke Foundation of Ontario and the Canadian Institute of Health Research for their financial support.

Last but certainly not least, a sincere thank to my parents, my brother and my friends for their continuous and essential support.

LIST OF CONTRIBUTIONS

Surgeries for pigs 1-7 (Surgeries 1,2,3): Dr. Munir Boodhwani

Surgeries for pigs 8-18 (Surgeries 1,2,3): Dr. Pingchuan Zhang

Surgeries for pigs 18- 33 (Surgeries 1& 2): Dr. Talal AlAtassi

Surgeries for pigs 15-33 (Surgeries 1 & 2: assisting): Céline Giordano

Surgeries for pigs 18-33 (Surgeries 3: surgeon) Céline Giordano & Dan de Vette

PET scan acquisitions for all pigs: Stephanie Thorn

PET scan acquisitions for pigs 16-33 (assisting): Céline Giordano

Echocardiography acquisition for pigs 1-26: Mike Blakeley

Echocardiography acquisition for pigs 26-33: Wilson Miranda & Kim Edwards

Microsphere analyses for pigs 1-16: Dr. Munir Boodhwani

Microsphere analyses for pigs 17-33: Céline Giordano

PET scan analyses for pigs 1-16: Jennifer Renaud

PET scan analyses for pigs 16-33: Céline Giordano

Echocardiography analyses for all pigs: Dr. Kathy Ascah

Cell isolation and preparation for injection; Randomization for all pigs: Suzanne Crowe

Matlab program & analyses for summed polar maps: Dr. Ran Klein

1. INTRODUCTION

1.1. Coronary artery disease

Coronary artery disease (CAD) is responsible for over 30 % of all deaths, both in the United States (AHA) and Canada (Statistic-Canada). The underlying process for CAD is the accumulation of atherosclerotic plaques within the intima of coronary arteries. Following an injury of the vessel endothelium, an inflammatory response is triggered, leading to migration and accumulation of low density lipoprotein (LDL) and monocytes in the intima. Activated monocytes further differentiate to macrophages and take up oxidised LDL, becoming foam cells. In response to pro-inflammatory cytokines, smooth muscle cells migrate, proliferate and form a fibrous cap over the foam cells ultimately leading to intima hyperplasia and atherosclerotic disease (Dzau *et al.*, 2002; Karatzis, 2005). As these plaques expand in the coronary artery walls, they obstruct the lumen of the vessels thereby impairing blood flow. Reduced blood flow to the myocardium leads to myocardial ischemia and may degenerate to clinical conditions such as chronic angina, myocardial infarction, heart failure and, ultimately, death. Current therapies such as coronary artery bypass grafting (CABG) or percutaneous coronary intervention are well established (Mukherjee *et al.*, 1999; Smith, 2009) but not suitable to all patients; in a previous study, over 1/3 of patients referred for revascularization did not undergo intervention because of unsuitable vessel anatomy, co-morbidities, or other reasons(Beanlands *et al.*, 1998). In addition, some patients may not benefit from such therapies in the long run (Mukherjee *et al.*, 1999; Ruel *et al.*, 2002). Alternate treatment options are therefore being researched, among which stimulation of angiogenesis through the administration of growth factors, genes or progenitor cells (Ruel *et al.*, 2004) could constitute a promising alternative or supplementation to actual therapies.

1.2. Myocardial ischemia and hibernation

Myocardial ischemia occurs when there is an imbalance between oxygen demands and supply. Two common conditions resulting from this imbalance are myocardial stunning and hibernation. Myocardial stunning is a state of fully reversible post-ischemic contractile dysfunction that persists even with normalisation of blood flow. Recovery of function can occur within hours or days. In dogs, contractile dysfunction recovered after 6 hours following a 5 min ischemia, whereas over 24h was needed to recover from a 15 min ischemic period (Heyndrickx *et al.*, 1975). Myocardial hibernation is a state of chronic systolic and diastolic dysfunction, progressively reversible after reperfusion (Rahimtoola, 1985). In contrast to myocardial stunning, recovery may take up to a full year in some patients, depending on the extent of ischemia and the underlying damages done to the myocardium (Depre & Vatner, 2007). The initial description of hibernating myocardium was based on clinical observations by Rahimtoola, who described myocardial hibernation as "a prolonged subacute or chronic stage of myocardial ischemia […] in which myocardial contractility and metabolism and ventricular function are reduced to match the reduced blood supply." (Rahimtoola, 1985). This description of hibernation was later called the *smart heart* hypothesis (Mari & Strauss, 2002), because alterations in function and metabolism were seen as a protective mechanism to reduce oxygen demands and maintain myocardial integrity and viability, rather than a consequence of ischemia. In contrast, the more recent *repetitive stunning* hypothesis attributes hibernation to repetitive episodes of ischemia, initially stunning the myocardium but progressively leading to a chronic state of contractile dysfunction. In opposition to the *smart heart* hypothesis, the reduction in blood flow is viewed as a consequence of hibernation rather than a cause. Regardless of the mechanisms leading to hibernation, pathophysiological analyses of hibernating myocardium consistently

show structural and metabolic changes in hibernating segments, reflecting what appears to be a combination of adaptative (Vogt *et al.*, 2003; Page *et al.*, 2008; Hu *et al.*, 2009) and degenerative changes (Schwarz *et al.*, 1998; Vogt *et al.*, 2003; Angelini *et al.*, 2007). The concepts of functional and structural hibernation (Camici & Dutka, 2001) were put forward to explain the divergence in functional recovery following revascularisation. Early and complete recovery likely occurs in patients with functional hibernation, when impaired blood flow was not prolonged enough to create myocardial damage, whereas later and/or incomplete recovery may occur when structural changes to cardiomyocytes appear. In line with this description, myocardial stunning and hibernation appear to be a continuum (Canty & Fallavollita, 2000), and hibernating, stunned and infarcted segments cohabit within a chronically hibernating heart (Hughes *et al.*, 2001).

Detecting hibernating myocardium in patients with CAD is important as timed revascularisation can improve wall motion, left ventricular ejection fraction (LVEF) and cardiac metabolism, in addition to preventing adverse left ventricle (LV) remodelling (Lai *et al.*, 2000; Allman *et al.*, 2002). Early revascularisation is also associated with more frequent improvements in LVEF and lower mortality rates (Beanlands *et al.*, 1998). On the other hand, failure to revascularise the territory at risk may lead to heart failure and sudden death (Beanlands *et al.*, 1998). Detection of the extent, in addition to the presence of hibernation is also desirable as no improvement in function is observed in regions with significant fibrosis or scar tissue (Rahimtoola *et al.*, 2006). The beneficial effects of revascularisation therefore depend on the severity of structural and metabolic changes in cardiomyocytes. Whether degeneration and apoptosis of cardiomyocytes is significant in hibernation remains debatable, but early revascularisation is highly warranted.

Various non-invasive techniques are available to detect regions that would benefit from revascularisation. They will be reviewed in section 4 with an emphasis on positron emission tomography, the gold standard for viability assessment.

1.3. Ameroid constrictor model of ischemia and hibernation

1.3.1. Swine as pre-clinical animals

For many decades, dogs were the most commonly used specie in studies of myocardial ischemia. In 1987, Maxwell *et al.* (Maxwell *et al.*, 1987) studied the variations in collateral flow between various mammalian species and found that dogs have substantial amounts of innate epicardial collaterals, as well as scattered collaterals in the deeper layers of the myocardium (Elsässer & Schaper, 1995). These innate vessels are capable of providing up to 40% of normal flow after acute coronary artery occlusion (Hearse, 2000). In the case of slow coronary occlusion, there is an intense and rapid proliferation of collateral vessels. For instance, when dogs are instrumented with an ameroid constrictor that causes gradual coronary occlusion, they rapidly develop collaterals which results in normal blood flow in the region at risk. Under drug-induced vasodilation, blood flow exceeds resting levels, indicating an important coronary flow reserve (Erbs *et al.*, 2005). Because of the many anatomical and physiological similarities between swine and human heart, most recent studies have favoured porcine models. A pig's heart has a limited innate collateral circulation, with only sparse endocardial connections (Unger, 2001). It responds to an ischemic stimulus by proliferation of blood vessels; however, these newly formed collaterals do not develop to the extent of restoring regular blood flow (White *et al.*, 1992) and are unable to restore normal perfusion to the area at risk, either under drug induced vasodilation

or exercise stress. They also lack a significant amount of smooth muscle cells compared to other arterial vessels (O'Konski *et al.*, 1987). In addition, unlike dogs that possess a two-vessel system with a non-dominant right coronary artery supplying only the right ventricle in a majority of animals, pigs have three major coronary vessels supplying the heart in a similar fashion to humans (Unger, 2001). A number of other similarities are worth mentioning: the swine heart metabolism is similar to that of humans, relying preferably on fatty acids under normal conditions, and switching to glucose during myocardial ischemia (Hughes *et al.*, 2003); and the heart size-to-body weight ratio (0.005) is identical to that of humans for pigs weighing around 30kg.

1.3.2. Ameroid constrictor model

First described by Litvak in the late 1950s (Litvak *et al.*, 1957) and further characterized by Shaper in the 1960s (Schaper, 1971) the ameroid constrictor model is one of the most widely used ischemia models. Ameroid constrictors consist of an inner hygroscopic casein core encased in a steel ring. When implanted around an artery, the inner hygroscopic material absorbs water and swells. Because outward expansion is prevented by the ring, swelling is directed inward slowly obstructing the vessel inside the constrictor lumen.

Ameroid constrictors have commonly been placed on the left circumflex (LCx) coronary artery, which is the smallest of the three coronary vessels in swine supplying approximately 20% of the LV (Hughes *et al.*, 2004). In addition, the innate collateral circulation is more important in the LCx compared to the left anterior descending (LAD) region, minimizing the risk of myocardial infarction and maximizing survival rates. Insertion

of the constrictor around the LCx artery is typically done by a small thoracotomy through the fourth or fifth intercostal space. Less invasive techniques such as thoracoscopy have successfully been used to place the constrictor around the LCx. Significant reductions in LVEF and fractional shortening (FS), as well as a low mortality rates were achieved using this technique (Zhu *et al.*, 2008; Chen *et al.*, 2009a).

Nevertheless, only few studies have specifically studied the development of myocardial hibernation in the ameroid constrictor model. In this regard, one aim of this study is to characterise the establishment of hibernation in this context, by using positron emission tomography.

1.4. Evaluation of myocardial function, perfusion and viability

Following revascularisation, an improvement in LV function and coronary flow reserve is hoped for. Various non-invasive techniques to evaluate function, perfusion and viability are available for clinical use. The most commonly used techniques to detect viability are summarized in Table 1. In their simplest application, echocardiography and magnetic resonance imaging (MRI) assess global and regional LV function. When used in conjunction with dobutamine, stress echocardiography (Wu & Lima, 2003; McLean *et al.*, 2009) and MRI (Bree *et al.*, 2006) can assess the contractile reserve of the heart, an indicator of viability. Positron emission tomography (PET) and single photon emission computed tomography (SPECT) are used to assess myocardial perfusion and viability at the cellular level (Maes *et al.*, 1997; Demirkol, 2008). Contrast enhanced echocardiography and MRI can also be used to evaluate perfusion and respectively the patency of microvasculature, reflecting viability (Camici *et al.*, 2008; McLean *et al.*, 2009) and the extent of scar or fibrotic tissue (Ibrahim *et al.*, 2005; Judd *et al.*, 2005). Newer techniques such

electromechanical mapping (NOGA mapping system) (Fuchs *et al.*, 2001; Gyongyosi *et al.*, 2001; Keck *et al.*, 2002) and strain and strain rate imaging (echocardiography-based) (Hoffmann *et al.*, 2005; Miyasaka *et al.*, 2005) are used to asses myocardial viability. In the experimental setting, labelled microspheres are commonly used to evaluate perfusion at a given time point (Prinzen & Bassingthwaighte, 2000).

Imaging technique	Detects
Cell viability	
SPECT	
• ^{201}Tl	Perfusion & cell membrane integrity
• ^{99m}Tc tracers	Perfusion, cell membrane/mitochondrial integrity
^{18}F-FDG PET	Glucose utilisation and transporter integrity
Contrast enhanced echo	Perfusion & microvasculature patency
Contrast-enhanced MRI	Perfusion & absence of cell membrane integrity
Electromechanical mapping	Electrical and mechanical activity of cells
Contractile Reserve	
Dobutamine stress echo	Improved function after inotropic stimulation
Dobutamine MRI	Improved function after inotropic stimulation
Strain rate echo	Deformation of the myocardium
LV morphology	
Echo	
MRI	

Table 1: Most common imaging techniques used to detect myocardial viability

1.4.1. General principles of PET

Positron emission tomography is a nuclear imaging technique considered the gold standard for non-invasive measurement of myocardial perfusion and viability. It uses isotopes that decay by emitting a positron and a neutrino. The positron travels a short distance in the tissue interacting with electrons until it has lost enough energy to annihilate with one single electron. This results in the emission of two 511-kev gamma photons 180° apart that are detected in coincidences by a ring of detectors on the PET camera. An image reconstruction algorithm is then applied to the signals, and radioactivity distribution information is retrieved (Townsend, 2004; Bengel *et al.*, 2009). Hence, the principle of PET is to follow radiolabelled probes (tracers) as they travel and are metabolised in the body. Information on perfusion, glucose and fatty acids metabolism can be obtained from PET imaging by using the appropriate tracer.

1.4.2. Perfusion imaging

Myocardial perfusion imaging is an important clinical tool to detect impaired coronary blood flow caused by narrowing of coronary arteries. Information retrieved rom it provides precious information on regional myocardial blood flow (MBF), which in turn can orient therapy to delay or reverse the development of atherosclerosis, to medically or surgically treat symptoms of ischemia and to prevent future events and improve patient survival (Dilsizian *et al.*, 2009).

The ideal tracer to evaluate perfusion would distribute in the myocardium proportionally to myocardial perfusion, have a high first pass extraction ratio with only minimal washout from the cells and eliminate rapidly from the muscle to allow serial

imaging. Although no tracer combining all previous characteristics is available, ^{13}N-ammonia (^{13}N-NH_3) is well suited to measure relative and absolute myocardial perfusion (Schelbert *et al.*, 1981; Khorsand *et al.*, 2005). From the blood where it is injected, ammonia first travels to the interstitial space. It then either passively diffuses across cell membranes or is actively transported into cardiomyocytes by the Na^+/K^+ pump. Once in the cells, ammonia can be retained as ^{13}N-glutamine or can diffuse back into the blood (Schelbert *et al.*, 1981). The cellular uptake of ammonia depends on myocardial blood flow, extraction ratio and retention rate. Ammonia's first pass extraction ratio from the blood is over 90% (Klein *et al.*, 2010a), but decreases as MBF augments: it is inversely and non-linearly related to MBF (Schelbert *et al.*, 1981). Based on the uptake and retention characteristic of the tracer, a kinetic model is developed to describe the exchange of tracer between the blood and the cells, thereby approximating absolute myocardial perfusion in millilitres per minute per gram of tissue (ml/min/g) (DeGrado *et al.*, 1996; Khorsand *et al.*, 2005). The absolute quantification of myocardial blood flow achievable by PET is certainly advantageous for patients with multiple vessel disease where global perfusion defect can hinder the detection of locally impaired perfusion (Parkash *et al.*, 2004).

To assess the ischemic status of the myocardium a rest and a stress scan are performed together. Because of the short physical half-life of PET tracers (^{13}N-NH_3: 9.8 min (Nitzsche *et al.*, 1996)) and the requirement for perfect anatomical match between rest and stress images, pharmaceutical stress agents instead of exercise are used. Coronary dilators such as adenosine and dipyridamole increase MBF in normal arteries, but only do so moderately in stenosed arteries (Ali Raza *et al.*, 2001). The ratio of stress

over rest MBF is myocardial flow reserve (MFR), an indicator of the vasodilation capacity of the arteries. Normal perfusion at stress typically rules out physiologically significant CAD and abnormal perfusion at stress suggests narrowing of the coronary arteries. If perfusion is restored at rest, reversible ischemia is present. On the other hand, if impaired perfusion persists at rest, there is irreversible damage to the myocardium (Dilsizian *et al.*, 2009)

1.4.3. Metabolic imaging

^{18}F-fluorodeoxyglucose (^{18}FDG)- PET (half life: 110 min (Fowler & Ido, 2002)) is considered the gold standard for myocardial viability imaging (Mari & Strauss, 2002). FDG is a glucose analogue that travels into the cells similarly to glucose. Upon its entrance into the myocytes, FDG is phosphorylated to FDG-6-phosphate and cannot undergo further metabolism. Because its rate of dephosphorylation is slow, FDG-6-phosphate remains trapped in the cells and radioactive decay of ^{18}F provides a strong signal for PET imaging. Absolute quantification of FDG uptake rate is possible, but not routinely done in the clinical setting because of high variability in regional glucose uptake between patients (Gerber *et al.*, 2001). The quality of FDG images is largely dependant on FDG uptake by the cardiomyocytes, which in turn depends on the dietary and diabetic status and the severity of ischemia (Camici *et al.*, 2008). Fasting state and glucose loading are used to drive FDG/glucose into the cells. However, in many patients the release of endogenous insulin does not induce maximal myocardial uptake of FDG/glucose (Iozzo *et al.*, 2002). A euglycemic hyperinsulinemic (insulin clamp) has been developed and positively tested (Gerber *et al.*, 2001). Glucose front load followed

by intravenous injection of insulin reduces plasma free fatty acids and causes a switch to glucose metabolism in insulin sensitive tissues. When FDG is injected, it is rapidly taken up by cardiomyocytes leading to better image quality. In addition to clinical use, this technique has been successfully used in pigs with hibernating myocardium (Fallavollita, 2000).

1.4.4. Imaging the hibernating myocardium with PET

Reduced myocardial perfusion at rest may reflect scarred or hibernating tissue. Myocardial perfusion imaging alone is therefore not sensitive enough to detect viable tissue from fibrous scar. When combined with metabolic imaging, PET can discriminate between normal, viable and scarred myocardium. In the healthy myocardium, normal perfusion and metabolism are present. In hibernating segments, cardiomyocytes switch from oxidative respiration to anaerobic glycolysis (Camici *et al.*, 1989), increasing glucose uptake and leading to increased intracellular glycogen contents (Borgers *et al.*, 1993; Borgers & Ausma, 1995; Vogt *et al.*, 2003). Because perfusion is reduced and viability maintained, hibernation appears as a perfusion-metabolism mismatch. In the same line, reduced perfusion matched to reduced metabolism indicates scar.

1.4.5. Microspheres

Microspheres are considered the gold standard for MBF measurements in experimental studies. They are 15 μm particles that were initially radioactively labelled but that are now coloured or tagged with a stable isotopes (Reinhardt *et al.*, 2001). Upon their injection into the left atrium, microspheres uniformly mix with the blood in the

ventricle and travel into the coronary arteries and capillaries within the blood volume. On their first passage after injection, they get trapped into arterioles and capillaries with a diameter inferior to 15 µm, thereby providing information on MBF at a given time Absolute MBF is calculated based on the number of microspheres in a tissue sample, relatively to their number in a reference blood sample drawn at a known rate. (Heymann *et al.*, 1977). ILM of different isotopic mass are available, allowing serial measurements of perfusion.

1.4.6. Echocardiography and dobutamine stress echocardiography

Basic echocardiography is used to evaluate LV morphology, which is important when evaluating the potential of recovery post revascularisation. For instance, patients with severely dilated LVs (Bax *et al.*, 2004), high left ventricular end-systolic volume (Bax *et al.*, 2004; Schinkel *et al.*, 2004) or decreased wall thickness are less likely to show improved function after revascularisation. Other parameters such as LVEF, FS and regional wall motion can be derived from echocardiography and used to assess basic heart function.

Dobutamine stress echocardiography is a well-recognized method to assess myocardial viability. It is based on the heart's response to positive inotropic agents that can transiently reverse dysfunctional contractility, such as dobutamine. A typical biphasic response is observed when viable myocardium is present: under low dose dobutamine infusion, segments with an abnormal wall motion react and contract better, leading to an improved contractile reserve. With a higher dobutamine dose a worsening in wall motion

is observed (Wu & Lima, 2003; McLean *et al.*, 2009). This biphasic response is specific to viable tissue, such that scar tissue does not respond to inotropic stimulation.

When used to predict regional recovery of function following revascularization, PET is the most sensitive method while DSE is the most specific one. When used to predict global recovery of function, PET had a higher sensitivity than DSE while no difference was observed in terms of specificity (Schinkel *et al.*, 2007)

1.5. Stem cell vasculogenic therapies

1.5.1. Endogenous angiogenesis, vasculogenesis and arteriogenesis

Angiogenesis, vasculogenesis and arteriogenesis are the three processes responsible for the growth of new blood vessels. Angiogenesis denotes the sprouting of newly formed capillaries from the sides and ends of pre-existing vessels via proliferation and migration of mature pre-existing endothelial cells (ECs). Vasculogenesis consists in the formation of new vasculature from an avascular structure via *in situ* migration, proliferation, differentiation and/or incorporation of bone marrow (BM) derived progenitor cells into the foci of neovascularization. Initially thought to be restricted to embryonic development, vasculogenesis is now accepted to participate in post-natal neovascularization. Arteriogenesis refers to the remodelling of pre-existing vessels resulting in new arteries (increased in size and calibre (Freedman & Isner, 2002)) possessing a fully developed tunica media (Post *et al.*, 2001). It may result from the maturation of pre-existing collaterals in response to a supply-demand imbalance (Ruel *et al.*, 2004) or *de novo* formation of mature vessels.

Under ischemic conditions, the natural tissue response is to stimulate an inflammatory process and increase the expression of pro-angiogenic factors in an effort to reduce ischemia. In the heart, this response pathway involves the hypoxia-inducible transcription factor HIF-1α. In normoxia, HIF-1α is expressed at high levels and continually degraded; in hypoxia, its degradation is inhibited leading to its accumulation and ultimately transcriptional activation of target genes such as vascular endothelial growth factor (VEGF) (Semenza, 2007; Krenning *et al.*, 2009; Kim *et al.*, 2011), stromal derived factor-1 (SDF-1) (Semenza, 2007; Krenning *et al.*, 2009), and angiopoietins (Semenza, 2007). The SDF-1α/ CXCR4 axis is one of the most potent triggers for mobilisation of progenitor cells from the BM. *In vitro* studies revealed a dose-dependant effect of SDF-1 on bone marrow cells (Yamaguchi *et al.*, 2003), and *in vivo* studies confirmed the importance of SDF-1 for recruitment, engraftment (Askari *et al.*, 2003; Yamaguchi *et al.*, 2003) and retention of BM cells in the ischemic myocardium.

Progenitor cells recruited from the BM secrete cytokines and growth factors (Kamihata *et al.*, 2001; Ii *et al.*, 2005; Miyamoto *et al.*, 2007), creating a pro-angiogenic environment and setting the stage for further sprouting of new blood vessels through angiogenesis. The initial steps of this process consist of the vasodilation of existing vessels and an increase in capillary permeability. This results from rearrangements in cell membrane structures and redistribution of intercellular proteins such as platelet endothelial cell adhesion molecule (PECAM-1) and vascular endothelial (VE)-Cadherin. Mainly mediated by nitric oxide (NO) and VEGF, it is followed by extravasation of plasma proteins, a process induced by VEGF but tightly regulated by angiopoietin 1 (Ang1; a natural anti-permeability factor and ligand for the endothelial receptor Tie2

(Thurston *et al.*, 1999)). Detachment of smooth muscle cells and degradation of the extracellular matrix is mediated by Ang2, (an inhibitor of Tie2 signalling and antagonist of Ang1 (Suri *et al.*, 1996; Maisonpierre *et al.*, 1997)) and metalloproteinases. Interestingly, CD14+ monocytic cells also appear to drill tunnels in the extracellular matrix, potentially serving as a template for capillary formation. These tunnels contain erythrocytes and are lined with CD14+ cells that are later replaced by Tie-2+ BM derived progenitors or mature ECs (Moldovan *et al.*, 2000; Anghelina *et al.*, 2006). As physical barriers are removed and inter-endothelial cell contacts relieved, ECs proliferate and migrate to distant sites (Gale & Yancopoulos, 1999), stimulated by the liberation of endogenous growth factors trapped in the matrix and released following its degradation (Conway *et al.*, 2001). ECs then assemble into tubules, acquire a lumen and re-express adhesion molecules such as VE-cadherin. Once the vessel has assembled, ECs become remarkably resistant to apoptosis and are quiescent with a very low turnover rate. These newly formed capillaries can either remain dormant or continue to develop into a mature functional vessel.

1.5.2. General principles of progenitor cell therapy

Progenitor cell therapy is a recent area of research that emerged from the discovery of the proliferative and differentiation capacity of stem cells. In the context of myocardial regeneration, the revelation that the heart was not a post-mitotic organ opened a new and promising area of research. The heart, in fact, possesses intrinsic repair mechanisms that involve proliferation of cardiomyocytes (although limited) (Beltrami *et al.*, 2001), homing of BM derived progenitor cells (following an ischemic injury) and

action of resident cardiac stem cells. Following an injury, this natural response is not sufficient to fully recover the myocardium and must be supplemented with an outside intervention to increase chances of recovery (Kodama *et al.*, 1996). Hence, the concept of cell therapy is to repopulate the myocardium with myogenic cells to restore the contractile function of the heart and/ or angiogenic cells to restore the vasculature. Transplanted cells can survive in the ischemic tissue, regenerate the vasculature, improve cardiac function and prevent LV remodelling. It was initially believed that cells improved function by transdifferentiation into cardiomyocytes or restored perfusion by incorporation into the vasculature. However, findings from additional studies showed that 1) only a small amount of cells really transdifferentiated to cardiomyocytes (Jackson *et al.*, 2001), if any (Balsam *et al.*, 2004; Murry *et al.*, 2004); 2) functional improvement following transplantation was visible after only 72h which cannot be attributed to regeneration induced by injected cells (Gnecchi *et al.*, 2006); and 3) only a small portion (1-10% (Hou *et al.*, 2005; Bartunek *et al.*, 2009)) of cells survived past 12h, whereas benefits of stem cell therapy were sustained longer (Gnecchi *et al.*, 2006). The current belief is that a paracrine mechanism mediates transplanted cells' effects, as it was shown that they can recruit host angiogenic cells (Kocher *et al.*, 2001), modify the local environment to induce the release of additional cytokines (VEGF, Ang-1, SDF-1) by the host tissue (Cho *et al.*, 2007), prevent apoptosis of host cardiomyocytes (Uemura *et al.*, 2006) and prevent matrix degradation and adverse remodelling (Fedak *et al.*, 2005; Formigli *et al.*, 2007).

1.5.3. Endothelial progenitor cells as vasculogenic mediators

The endothelial progenitor cell (EPC) is a bone marrow derived cell first identified in 1997 by Asahara *et al.* (Asahara *et al.*, 1997). They observed that the CD34 enriched fraction of BM mononuclear cells (MNC) had the ability to differentiate to ECs *in vitro.* Rapidly, these cells were extensively studied, which led to confusion on the definition and characteristics of EPCs. When used in the broad term, EPC refers to a population of circulating cells that promote revascularisation in ischemic, hypoxic or injured tissue, and that closely relates to various diseases. A number of protocols have been used and claimed to isolate the so-called EPC population. They consist of either the direct isolation of CD133, CD34 and VEGFR-2 triple positive cells (Peichev *et al.*, 2000), or the *ex vivo* culture of the mononuclear fraction of peripheral blood (PB) and subsequent EPC isolation. However, the true EPCs are circulating cells that have the ability to clonally give rise to a progeny capable of forming endothelial tubes *in vitro* and spontaneously contribute to the formation of functional endothelium *in vivo* (Lin *et al.*, 2000; Yoder *et al.*, 2007; Melero-Martin *et al.*, 2008). These true EPCs form colonies after 7-21 days in culture, and are therefore referred to as endothelial colony forming cells (ECFCs). Only one single protocol yields ECFCs (Hirschi *et al.*, 2008).

When MNCs are plated on fibronectin for a short period (4-9 days), the adherent population was shown to actively contribute to neovascularisation and to be related to certain disease states. Because these cells are not true EPCs, they are often referred to as circulating angiogenic cells (CAC) (Rehman *et al.*, 2003). CACs constitute a highly heterogeneous cell population, encompassing cells that express endothelial markers (VEGF receptor 2; (VEFG-R2), CD34, von Willebrand factor (vWF); endothelial nitric

oxide synthase (eNOS), VE-Cadherin, etc.), but that also co-express markers suggestive of a hematopoietic origin (CD45, CD14, CD115) (Prater *et al.*, 2007). Nevertheless, these CACs play an important role in pathogenesis and prognosis of cardiovascular diseases. Increased numbers are associated with improved vascular function and recovery following a cardiac event (Lev *et al.*, 2005; Steiner *et al.*, 2005), whereas reduced numbers and migratory potential are observed in patients with CAD (Vasa *et al.*, 2001). There is, in addition an inverse correlation between the number of CACs and combined CAD risk factors (Hill *et al.*, 2003). In fact, patients with higher levels of CACs have a decreased risk of cardiovascular death, revascularisation or hospitalisation (Werner *et al.*, 2005).

Similarly to their endogenous behaviour, transplanted CACs can migrate into the ischemic myocardium and contribute to revascularisation mainly through their paracrine effects. When injected into the coronary circulation, only 3-5% (Hou *et al.*, 2005; Penicka *et al.*, 2005) of cells home to the area of ischemia, whereas early retention rates are higher with direct intramyocardial or transendocardial injection (up to 11% (Hou *et al.*, 2005)). CACs have been used in a number of pre-clinical animal studies including rodent models of hind limb (Kalka *et al.*, 2000) and myocardial ischemia/ infarction (Kawamoto *et al.*, 2001; Suuronen *et al.*, 2007; Schuh *et al.*, 2008). In both cases, neovascularization was observed, and improved left ventricular function with reduced infarcted size was achieved in models of infarcted myocardium.

Two groups have investigated the therapeutic effect of CACs (referred to as EPCs in the articles) in swine ameroid constrictor model. In light of the lack of consistency in EPC characterization and definition, the two studies used distinct culture protocols.

Kawamoto *et al.* (Kawamoto *et al.*, 2003) first isolated the $CD31^+$ fraction of MNCs using the MACS beads selection method, and further cultured them on non-coated dishes to remove adhesive macrophages. The non-adhesive $CD31^+$ cells ($NA/CD31^+$) were considered as the EPC enriched fraction. The $CD31^-$ cells ($NA/CD31^-$) were treated similarly and served as a negative control. *In vivo*, $NA/CD31^+$ but not $NA/CD31^-$ were successful in reducing the ischemic area and increasing angiography Rentrop scores, LVEF and capillary density. Chen *et al.* (Chen *et al.*, 2009b) isolated EPCs using the protocol of selective adhesion on fibronectin. MNCs were plated on fibronectin-coated dishes, non-adherent cells were removed after 4 days and cells were further expanded *in vitro*. EPCs were then genetically modified to express fibroblast growth factor 1 (FGF-1; Td/FGF-1-EPCs). *In vitro*, Td/FGF-1-EPCs showed increased viability, migration and tube formation, and secreted FGF-1 for at least 21 days after transduction. *In vivo*, their transplantation reduced rest myocardial perfusion defect evaluated by SPECT and yielded increased vessel density. Non-modified EPCs did not yield any improvement.

1.5.4. Limitations to progenitor cell therapy

Although being very promising, progenitor cell therapy faces many limitations and questions that need to be addressed to obtain optimal benefits. In the past ten years, many cell types have been evaluated in animal or clinical studies. Total BM-MNC were the first to be used in a clinical setting: despite promising pre-clinical evaluation, only modest benefits were obtained clinically (Abdel-Latif *et al.*, 2007; Wen *et al.*, 2011). Selected populations like CD34+ hematopoietic stem cells or mesenchymal stem cells were also tested in the clinical setting, yielding similar results to total BM-MNC. More

recently, induced pluripotent stem cells (iPS) and resident cardiac stem cells (CSC) were shown to be suitable for angiogenic therapies in animal models (Beltrami *et al.*, 2003; Wang *et al.*, 2006; Bearzi *et al.*, 2007; Gonzales & Pedrazzini, 2009). Early stage clinical trials addressing safety and feasibility (clinicaltrials.gov: NCT00474461) and Phase I randomized dose escalation trials (clinicaltrials.gov: NCT0089336) are underway for CSC. Nevertheless the ideal cell type, if it exists, remains to be identified. Similarly, the ideal cell concentration and number is unknown, as well as the ideal time for transplantation (Kuraitis *et al.*, 2010). Stem cell therapy also faces the presence of dysfunctional progenitors and pathologies such as endothelial dysfunction that can alter the status of autologous progenitor cells. To counter this limitation, current research aims at genetically modifying cells (Penn & Mangi, 2008) to express angiogenic factors such as FGF-1 (Chen *et al.*, 2009b) or angiopoietin-1 (Chen *et al.*, 2009a). As previously discussed, low viability and engraftment after transplantation urges the discovery of new strategies to prevent relocation and apoptosis of injected cells. In this regard, the use of tissue engineering by combining implantable biomaterials with easily available circulating angiogenic progenitor cells is promising.

1.6. Enhancing progenitor cell delivery with hydrogels

1.6.1. General principle

As previously described, progenitor cell therapy is hindered by low survival and engraftment of transplanted cells. One additional limitation is the migration of delivered cells to non-target sites (Suuronen *et al.*, 2008), potentially favouring the growth of unwanted tissues in unwanted locations. Tissue engineering through the use of 3

dimensional (3D) biomaterials has the potential to enhance cell therapy particularly by increasing survival, retention, and function of transplanted cells. The general concept of tissue engineering in stem cell therapy is to combine cells and 3D constructs to enhance and direct cell culture, or to use as a vehicle for transplantation, ultimately aiming at improving regeneration of damaged tissues. Ideally, the 3D material should mimic the extra-cellular environment it is intended to replace (de Mel *et al.*, 2008). It should also attempt to match the host tissue mechanical properties and provide structural and mechanical support during regeneration. In addition, it should enhance cell adhesion and survival as well as support the growth of new tissue. Engineered matrices are also required to be biocompatible (no rejection or induction of an adverse inflammatory response) and biodegradable (Jawad *et al.*, 2008). Compared to synthetic materials, natural biomaterials have the advantage of being made of endogenous components, minimising negative host responses (Langer & Tirrell, 2004). In this regard, the use of biomaterials engineered with extracellular matrix or extracellular matrix components are of great interest.

1.6.2. Collagen-based matrices

The extracellular matrix (ECM) of the heart is primarily composed of members of the collagen family, in particular collagen I, III and IV. Both collagen I and III assemble into fibrils and maintain the structural integrity of the ECM. Collagen I accounts for 80-90% of the total collagen in the heart and is an attractive molecule for tissue engineering involving regeneration. The arrangement of its fibres allows for the development of various pore sizes that are conducive to inward cell mobilisation. In addition, collagen is

adhesive to many cell types and provides a structure to the ECM and the engineered matrices as well as a scaffold for cells, preventing excessive stretching or slippage of cardiomyocytes (Hein & Schaper, 2001). *In vitro*, collagen can support the adhesion and the proliferation of endothelial and smooth muscle cells (Boccafoschi *et al.*, 2005).

When used in regenerative studies, collagen-based matrices were shown to improve LV function (Kutschka *et al.*, 2006) and capillary density (Huang *et al.*, 2005), enhance the survival of transplanted cardiomyocytes as evidenced by bioluminescence (Kutschka *et al.*, 2006), and reduce the relocation of transplanted cells (Dai *et al.*, 2009).

Our group has used a collagen I hydrogel supplemented with chondroitin sulfate. Hydrogels are defined as hydrated 3D networks. They can respond to various stimuli and gel upon their interaction/exposure *in vivo*. These include pH changes, ionic cross linking, crystallisation or temperature change (Wu *et al.*, 2009). Thermosensitive hydrogels such as the ones used by our group are liquid upon injection and solidify when exposed to physiological temperature. This allows initial dispersion of the matrix within the target tissue followed by entrapment of the delivered cells, preventing cell loss to non-target sites. Our matrix was successfully used to deliver CACs and improve their incorporation into vascular structures (Suuronen *et al.*, 2006a), as well as enhance their retention within the target tissue (Zhang *et al.*, 2008). Recently, *in vitro* work showed that culture of PB-MNC on our matrix yielded a highly potent angiogenic population (Kuraitis *et al.*, 2011). Finally, the development of a collagen-based matrix containing sialyl Lewis^X, a ligand for L-selectin enhanced the mobilization of endogenous CACs, and the recruitment of both endogenous and transplanted cells, increasing arteriole density and perfusion (Suuronen *et al.*, 2009) in a rat model of hindlimb ischemia.

1.7. Objectives and Hypothesis

1.7.1. Objectives

The objective of this research was to better characterise the angiogenic and repair potential of autologous CACs and the additional benefits conferred by their delivery within our collagen-based matrix in a relevant pre-clinical swine model of myocardial hibernation. In particular our objectives were to:

1- Develop a swine model of myocardial hibernation by placement of an ameroid constrictor around the LCx, and validate this model by evaluating:
   a. Myocardial ischemia with PET and microspheres
   b. Glucose metabolism (hibernation) with PET
   c. LV function with echocardiography.

2- Compare the angiogenic potential of CACs delivered in a collagen-based matrix *vs.* CACs alone *vs.* control, by evaluating:
   a. Myocardial blood flow at rest and stress with microspheres and PET
   b. Glucose metabolism and hibernation status (mismatch scores; PET)
   c. LV function with echocardiography
   d. Arteriole density with immunochemistry (follow-up only)

3- Compare absolute perfusion measured by PET and microspheres

1.7.2. Hypotheses

Our hypotheses were that:

1- Placement of the ameroid constrictor would create a stable model of myocardial ischemia and myocardial hibernation

2- Delivery of CACs would:

   a. Improve myocardial blood flow

   b. Restore glucose metabolism (reduce mismatch)

   c. Improve LV function

   d. Increase arteriole density

3- Delivery of CACs+matrix would yield greater improvements than CACs alone

4- MBF measured by PET would be related to MBF measured by microspheres

2. MATERIALS AND METHODS

2.1. General experimental sequence

All experimental procedures were performed with the approval of the University of Ottawa Animal Care Committee in accordance with the National Institute of Health's Guide for Care and Use of Laboratory Animals.

Thirty-three 8- to 10-kg female Yorkshire swine underwent ameroid constrictor implantation around the LCx artery. Two weeks later, all pigs underwent: 1) blood harvest for CAC isolation; 2) transthoracic echocardiography, 3) rest dynamic ^{13}N-NH_3 PET scan, 4) dipyridamole induced stress dynamic ^{13}N-NH_3 PET scan, 5) and rest dynamic ^{18}FDG PET scan. The following week, animals were randomized to intramyocardial injections of phosphate buffered saline (PBS) alone (control; n= 10), CACs (n=8), or the combination of CACs + collagen-based matrix (n= 7). In the two groups that received cells, a mean of $32.7\pm3.9\times10^6$ cells was used. At the same time, microsphere analysis of MBF was performed at rest and under dipyridamole induced stress. All animals underwent a follow-up imaging and echocardiography session at week six. The following week (week seven), a final rest and stress microsphere MBF measurement was done and animals were sacrificed. The heart was harvested for histophathological analyses and microsphere counts (Figure 1). This study was designed in a randomized blinded fashion. Animals were randomly selected to receive one of the two treatments or the control injection, independently of any physiological parameter. In addition, analyses were performed by blinded observers, and study groups were only revealed upon completion of all analyses.

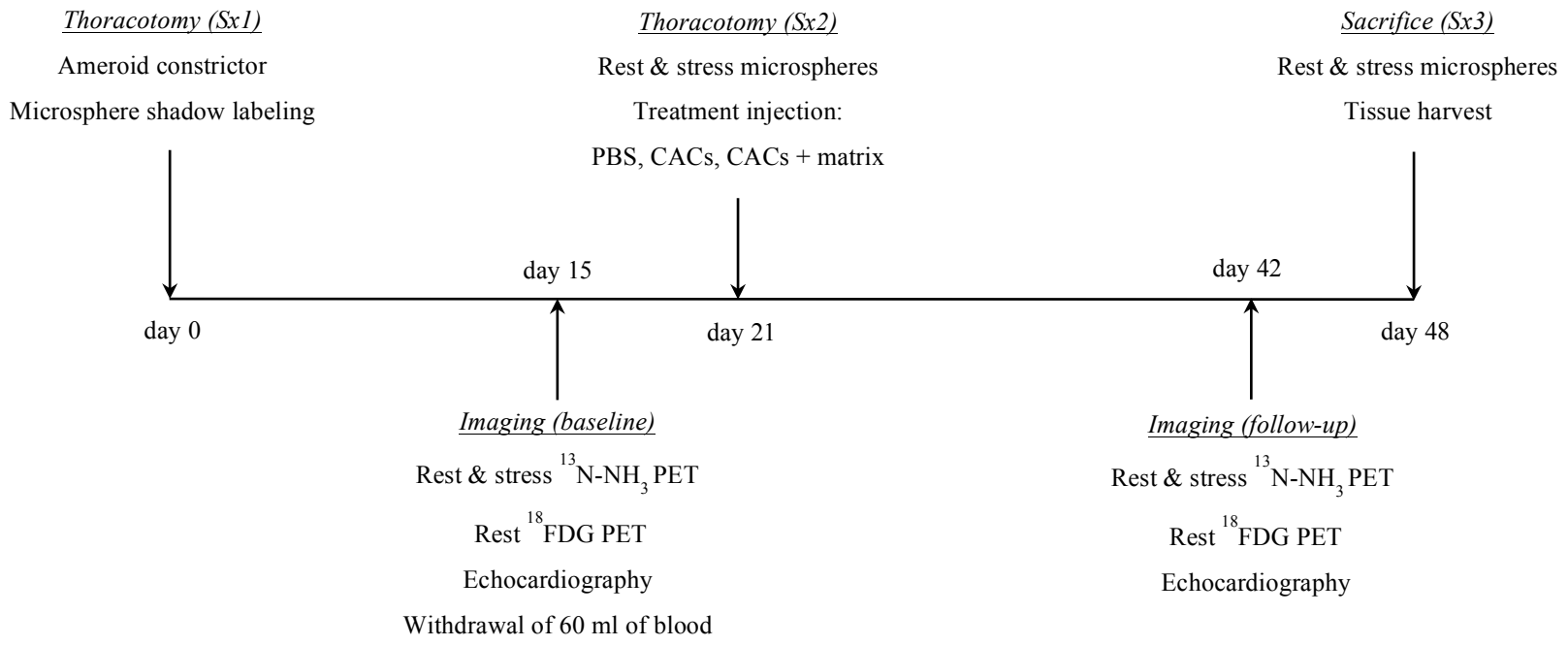

Figure 1: General experimental design

2.2. Surgical procedure

Pigs were anesthetised with a mixture of midazolam (0.5 mg/kg) and ketamine (11 mg/kg) and maintained with 0.75-3% isoflurane. This protocol was followed for the 3 surgeries and 2 imaging sessions. Buprenorphine (0.03 mg/kg) was administered before and after surgery or as needed. Animals were intubated and mechanically ventilated at 12-20 breaths per minute. At surgery one, a 4-5 cm left thoracotomy was performed. The pericardium was opened and the coronary groove exposed by retraction of the atrial appendage. The proximal LCx was carefully isolated and two vessel loops were placed around the artery (Figure 2A). Microsphere shadow labelling was performed during a 2-minute occlusion of the LCx artery to identify the area supplied by the left circumflex artery. Following the 2 minutes, nitroglycerine was sprayed on the artery for vasodilation, and the ECG was allowed to normalise before proceeding. An ameroid constrictor (1.5-2.0 mm; Research Instruments SW, Escondido, USA) was then inserted around the vessel upstream of the first marginal branch, and it was visually confirmed that the device did not acutely constrict the artery (Figure 2B). The ribs were brought together, the muscle layer was closed and the incision was closed with absorbable sutures in a subcuticular fashion. Three weeks after the first surgery, the animals underwent a second left thoracotomy *via* the original incision. The lateral wall of the heart was exposed to allow direct intramyocardial treatment delivery. A small incision was also made in the groin area, and a femoral artery catheter was inserted. Simultaneously to each microsphere injection in the atrium, an arterial blood sample was collected from the catheter for microsphere analyses. The femoral catheter was removed and the artery ligated. The incision was closed as described previously. Seven weeks after the first surgery, animals

were anesthetized and a median sternotomy was performed. Adhesions were dissected for direct access to the left atrium. Similarly to surgery 2, an arterial catheter was inserted into the femoral artery for microsphere reference blood sample harvest. Microspheres were injected in the left atrium under rest and dipyridamole induced stress while the reference blood sample was collected. Pigs were euthanized by exsanguination and the heart was harvested, washed under running water and sliced for microsphere and immunohistochemical analyses. Three sham animals underwent the same procedure with the exception of the insertion of the constrictor around the LCx. All subsequent steps were identical.

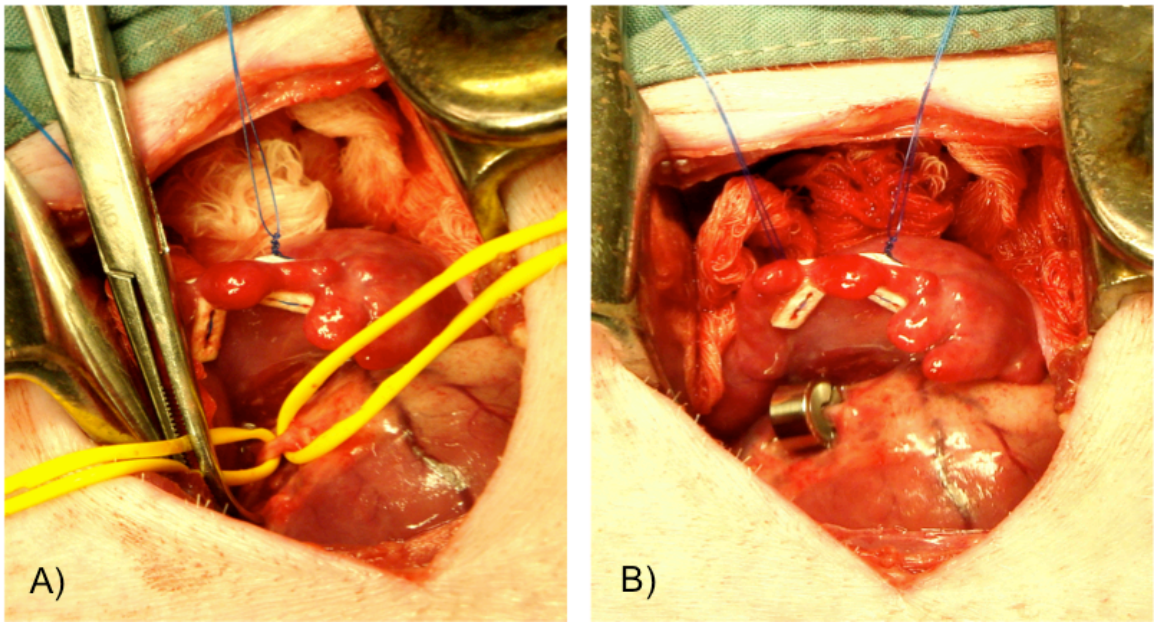

Figure 2: The ameroid constrictor. During a left mini thoracotomy, the left circumflex coronary artery was isolated between two vessel loops (A) and an ameroid constrictor was inserted around the artery (B).

2.3. Circulating angiogenic cell isolation and culture

Under sterile conditions, approximately 60 ml of arterial blood was harvested from a femoral artery branch and collected in ethylene diamine tetraacetic acid (EDTA)-containing Vacutainers (Greiner Bio-One, North Carolina, USA). MNC were layered on Histopaque 1077 (Sigma-Aldrich, Oakville, Canada) and centrifuged for 30 minutes at 800 × g (2000 rpm). The plasma layer was removed, and the buffy coat collected. It was subsequently washed with washing buffer (1.5 ml foetal bovine serum (FBS); 2.5 ml of EDTA and 150 ml of PBS (Sigma Aldrich, Oakville, Canada) and centrifuged at 450 × g (1400 rpm) for 10 minutes. The supernatant was removed and this washing step repeated twice. Following the last centrifugation, cells were resuspended in Endothelial Basal Media (EBM-2; Clonetics, Guelph, Canada) supplemented with EGM-2-MV-SingleQuots (Clonetics, Guelph, Canada) and counted with an automated Vicell™ Cell Viability Analyzer/Cell Counter (Beckman Coulter; Miami, USA) using the trypan blue exclusion method. Culture dishes were covered with approximately 2 ml of 0.1% human fibronectin for coating (Sigma Aldrich, Oakville, Canada). After 30 minutes, the fibronectin was removed and plates were washed 2 times with PBS. Approximately 20 million MNC were plated on each fibronectin-coated dish. EGM (10 ml) was added to the dish, and cells were cultured for 6 days at 37°C with 5 % CO_2 in a humidified atmosphere. After 4 days, non-adherent cells were removed by washing with PBS and 10 ml of new media was applied. On the day of injection, culture media was removed and cells were incubated with 1 ml of 1% trypsin for 8 minutes at 37°C. The same amount of EGM was added to the plate to stop the effects of trypsin and cells were lifted from the culture plate by repetitive washes with PBS. They were brought to a pellet by

centrifugation at 450 × g for 10 minutes. The supernatant was removed and CACs were resuspended in PBS. For the direct CAC injection, the pellet was resuspended in 3 ml of PBS. When mixed to the collagen matrix, cells were not resuspended and were directly added to 3 ml of matrix.

2.4. Collagen Matrix Preparation

Collagen-based matrices were prepared on ice by blending neutralised type I rat tail collagen (0.4% [w/v]; BD Bioscience, Oakville, Canada) with 20 % (w/v) chondroitin-6-sulfate. Glutaraldehyde (1.5%) served as a cross-linker and residual aldehyde groups were inactivated by the addition of glycine. The pH was adjusted to 7.2-7.5 and cells were added to the preparation. Everything was kept on ice until injection; this preparation is liquid at 4°C but solidifies at 37°C.

2.5. Dipyridamole-induced stress protocol

MBF measurements by microspheres and PET were performed under rest and stress conditions. Myocardial stress was induced by continuous injection of dipyridamole (0.56 mg/kg) over a 4-minute period. Exactly 4 minutes post total injection, ^{13}N-NH_3 was injected and the stress scan was started. In surgery, blood pressure was allowed to stabilise before injection of microspheres. Phenylephrine (10 μg/min – 60 μg/min; dose to effect) was administered as needed to prevent blood pressure drop (Fallavollita *et al.*, 2001).

2.6. Positron emission tomography

All animals underwent PET to determine MBF flow and metabolism. This was performed 2 weeks following constrictor implantation (baseline) and 3 weeks after treatment administration (follow-up).

2.6.1. Imaging sequence

Following an overnight fast, pigs were anesthetised, intubated, mechanically ventilated, and placed in a right lateral position on the bed in one of the following PET scanners: ECAT ART (Siemens), Discovery RX or 690 (General Electric) (Figure 3 B & C). A 12-lead ECG was used to monitor the heart (Figure 3A). Following a low-dose ^{137}Cs transmission (Townsend *et al.*, 1999) or X-ray CT (Kemp *et al.*, 2006) scan for attenuation correction (AC), each animal underwent rest and dipyridamole stress (0.56 mg/kg) imaging with ^{13}N-ammonia (20 min) (Burwash *et al.*, 2008) and rest imaging with ^{18}F-FDG (60 min) (Vitale *et al.*, 2001) to obtain regional estimates of MBF (ml/min/g) and glucose uptake (MBq/cc) respectively. Each acquisition was dynamic and was separated by a 40 min period to allow decay of ^{13}N-ammonia activity. For each scan, radiotracers were injected via an ear catheter using a syringe pump (infusion time 30 s; volume 10 ml), and all activity residuals were flushed from the intravenous line at the end of infusion using an additional 10 ml saline. The total activity injected was approximately 200-550 MBq for ammonia scans and 150-300 MBq for FDG scans (dose by weight; approximately 15 kg at scan 1, and 40 kg at scan 2). To increase myocardial glucose uptake and image quality on the FDG scans, a euglycemic hyperinsulinemic clamp was used(Fallavollita, 2000). Following a 10 minutes 20% Dextrose front load (Baxter, Mississauga, Canada), insulin (Novolin®ge Toronto, Novo Nordisk, Mississauga,

Canada; dose = weight (kg)×0.25 IU in 50 ml of saline) was administered for 4 minutes at a rate of 48 ml/min. At the end of the 3rd minute, FDG was injected and the scan started. Insulin injection rate was lowered to 24 ml/min for 3 minutes and stabilised at 12 ml/min for the rest of the scan. Insulin was stopped 10 minutes prior to scan completion. Glycaemia was closely monitored for the full length of the scan; adjustments were done by altering the rate of glucose administration (Figure 4).

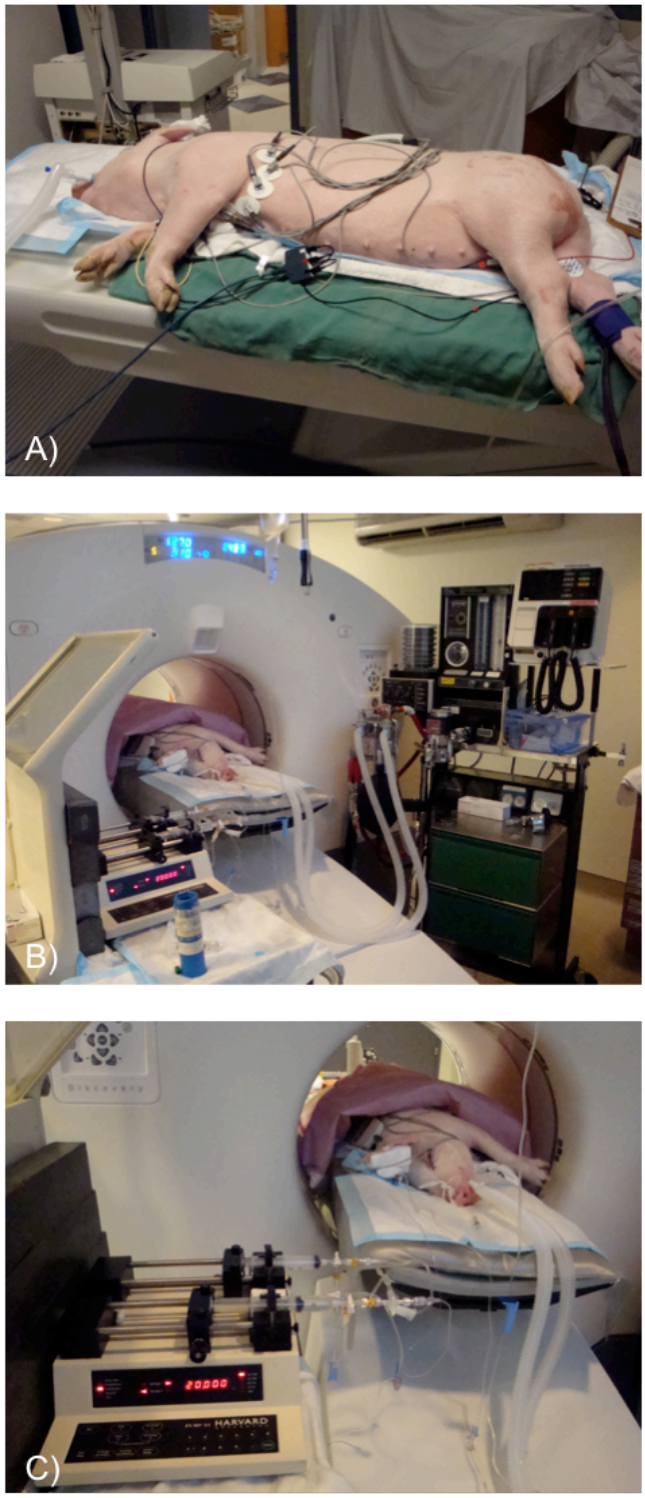

Figure 3: PET scans. Animals were positioned in a right lateral position and a 12 lead ECG was used to monitor the heart (A). All animals were under anaesthetics and mechanically ventilated (B). Ten millilitres of tracer was injected for each scan using a Harvard pump. Tracer injection was followed by a 10 ml saline flush to prevent accumulation of radioactivity in the line.

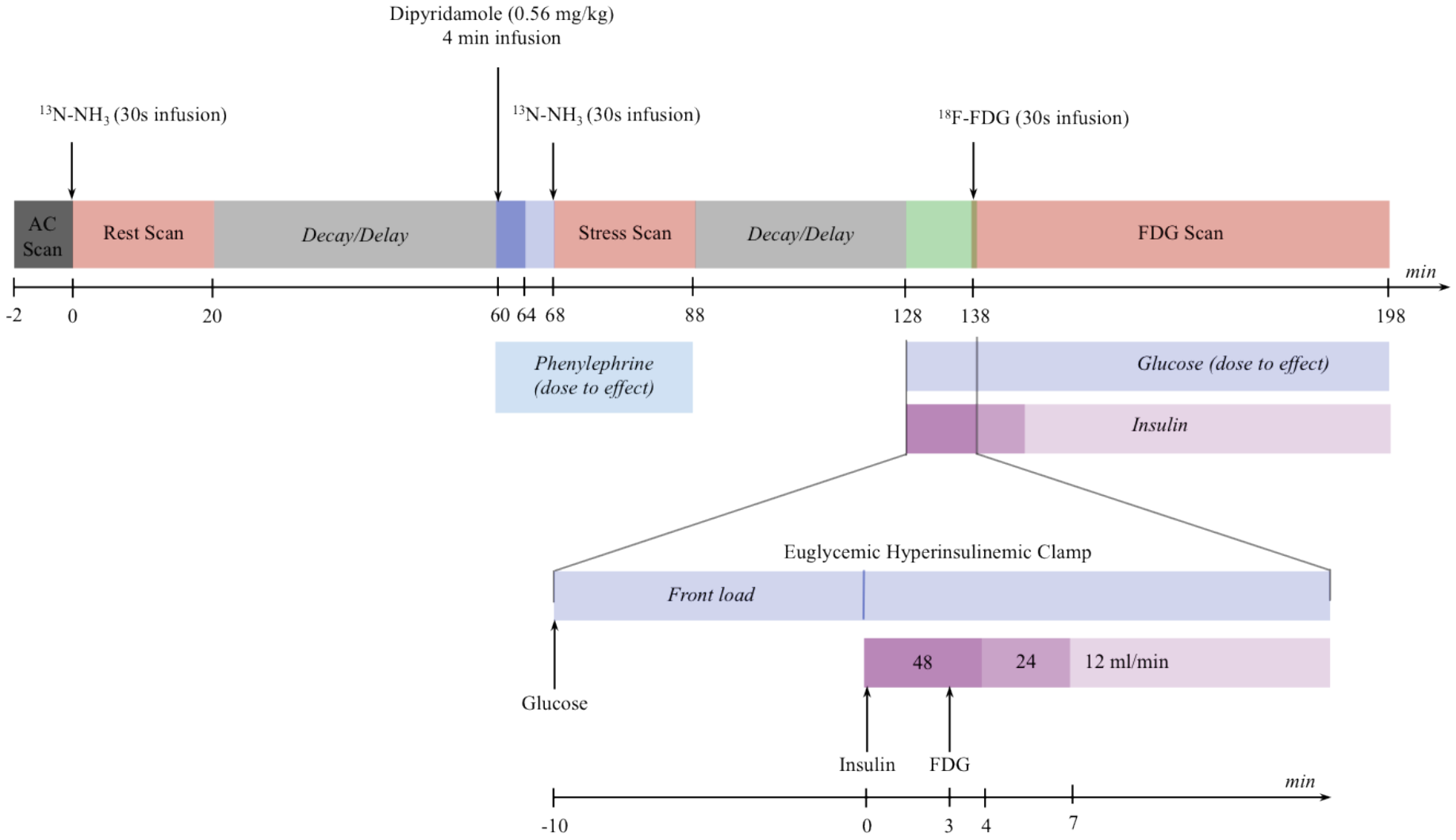

Figure 1: ^{13}N-NH$_3$ and ^{18}F-FDG image acquisition protocol.

2.6.2. Image processing

Images were processed using FlowQuant (Klein *et al.*, 2010b) (Ottawa, Canada), our in-house developed program. For MBF quantification, time activity curves were derived from sampling regions of interest in the myocardium and LV cavity, base and atrium blood pools. The rates of ^{13}N-NH_3 uptake at rest and stress were quantified using a one-compartment model (DeGrado *et al.*, 1996). Absolute MBF (ml/min/g) was quantified and reported according to a standard 17 segment-model (Figure 5) (Cerqueira *et al.*, 2002).

Mismatch analyses were performed by comparing relative NH_3 and FDG uptake at rest, as previously described (Beanlands *et al.*, 2002). Briefly, the LV was divided in 460 sectors and each sector was expressed as a % of the maximum tracer uptake, defining perfusion and FDG scores. Mismatch (hibernating myocardium) is defined in a segment with reduced perfusion with FDG score > perfusion. A match defect representing scar tissue is defined in regions where FDG score ≤ perfusion (Schelbert *et al.*, 2003). Mismatch and match scores were also reported following a 17 segment model.

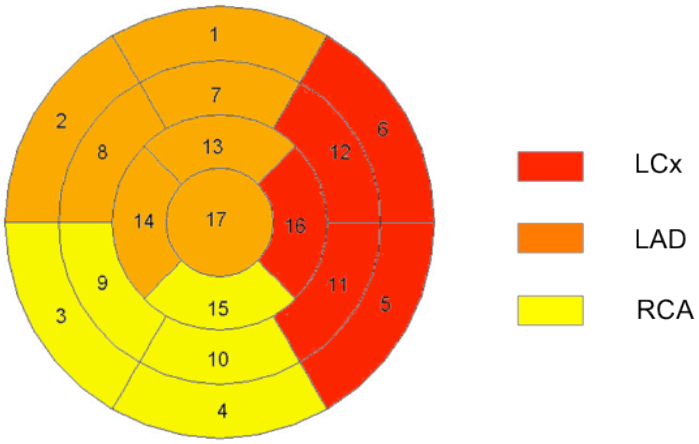

Figure 5: **Polar map representation of the left myocardium**. The polar map is divided in 17 segments and each segment is attributed to one coronary artery. LCx: Left circumflex; LAD: Left anterior descending; RCA: Right coronary artery.

2.6.3. Segment selection for MBF and viability analyses

To evaluate the development of ischemia and hibernation 2 weeks after ameroid placement, the LCx territory (segments 5, 6, 11, 12 and 16) was systematically compared to the remote LAD region (segments 1, 2, 7, 8, 13, 14 and 17) in each animal. To study the effect of each treatment, 2 adjacent segments were selected and their average value was used. For rest MBF, stress MBF and MFR, the 2 adjacent segments with the lowest MBF at stress within the 5 LCx segments were selected. For the remote region, two adjacent segments with the highest stress MBF were selected among 6 LAD contralateral segments (no apex; 17). For metabolic analyses, the 2 adjacent segments within the LCx territory with the highest mismatch score at baseline were selected. Control segments were selected in the LAD territory (no apex; 17) based on the lowest mismatch score. The same segments were used for match analyses.

2.7. Echocardiography

Rest transthoracic echocardiography images were acquired 2 weeks after ameroid constrictor implantation for baseline measurements of LV function, and 3 weeks after treatment administration for follow-up measurements. Standard parasternal long and short axis views, as wells as apical two and four chambers views were recorded with a Phillips Sonos 5500 ultrasound machine and analysed with Xcelera (Philips Healthcare, Andover, USA). From the M-mode measurements, LVEF was determined using the Teichholz method. Regional wall motion was evaluated by visual analysis of systolic thickening and reported following the 16-segment model recommended by the American Society of Echocardiography (Schiller *et al.*, 1989). A normal or hyperkinetic segment was assigned a score of 1, hypokinetic: 2, akinetic: 3, dyskinetic: 4. Wall motion score

index (WMSI) was calculated by dividing the total wall motion score in each animal by the number of segments visualised (16).

2.8. Protocol for heart slicing

Two 1.5 cm slices were cut at the midventricular level of the LV (Figure 6A). Each one was additionally sliced in 6 transmural sections starting from the anterior junction of the right and left ventricle (LAD territory). Samples were identified clockwise from 1 to 6 starting from the LAD. Only one septal segment was used; the rest of the septum and the right ventricle were discarded (Figure 6B). Approximately 1g of tissue from each section were used for microsphere analyses. Samples from the LCx4 territory were collected, fixed in 4% paraformaldehyde for 24h and used for immunohistochemistry. The ameroid constrictor was harvested and immediately fixed in 4% paraformaldehyde.

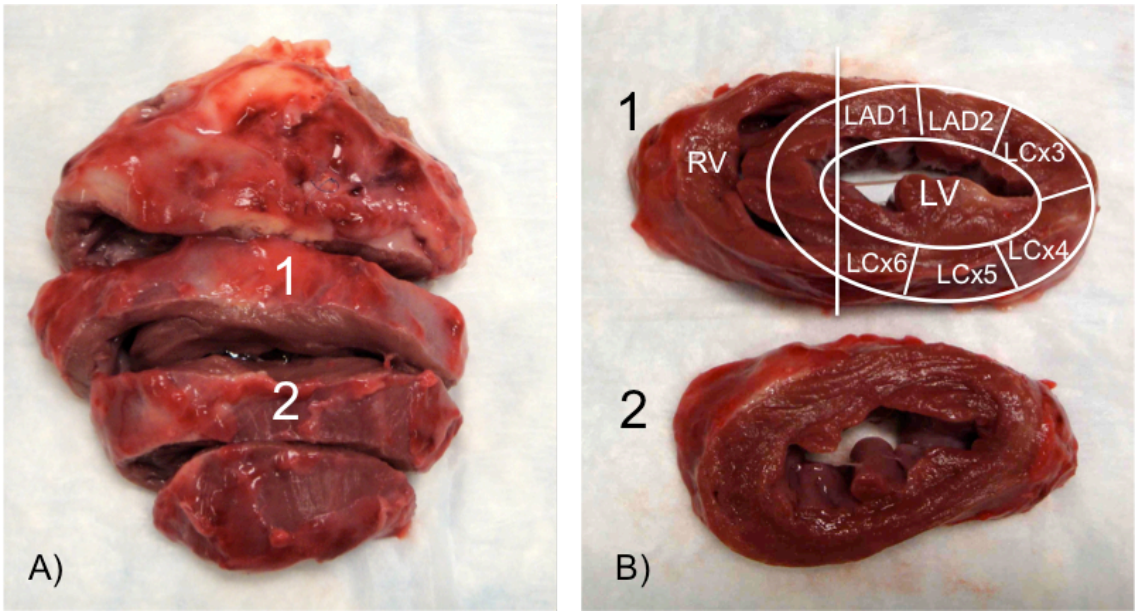

Figure 6: Heart preparation for microsphere and histology analyses. Following euthanasia, the heart was harvested for microsphere and histopathological analyses. Slices 1 and 2 were isolated (A) and cut as described in (B). For microsphere analyses, sections of approximately 1g were collected from all 6 territories and dried in a 60°C oven for 24h. For histopathological analyses, sections from the LCx4 territory were collected and fixed in 4% paraformaldehyde for 24h.

2.9. Myocardial blood flow determination with microspheres

MBF was assessed at surgeries 2 and 3 by using isotope-labelled microspheres (ILM; BioPAL, Worcester, USA). A total of 12.5 million ILM of different isotopic mass were used for each measurement. For accurate MBF measurements, a minimum of 400 to 600 microspheres is required per tissue segment. The number of microsphere (Y) was calculated using the following formula: $Y = (1.2 \times 10^6) + (1.9 \times 10^5 \times \text{mass of subject's (kg)})$ (Buckberg *et al.*, 1971; von Ritter *et al.*, 1988). However, because blood flow was reduced through the LCx, a higher number of microspheres was injected to ensure a total of 400-600 microsphere per tissue sample.

At the time of ameroid placement, 12.5 million ytterbium-labelled microspheres (15 μm) were injected in the left atrium over 30 seconds during temporary occlusion of the LCx to determine the myocardial area supplied by this artery (shadow labelling) (Figure 7A). For MBF determination, 12.5 million microspheres (15 μm) were injected in the left atrium over 30 seconds while a reference blood sample was drawn from the femoral artery at a rate of 8 ml/min. Lutetium and europium-labelled microspheres were used during the second procedure to determine MBF at rest and stress respectively, 3 weeks after ameroid placement. Lanthanum and samarium-labelled microspheres were injected during the final surgery to respectively evaluate follow-up MBF at rest and stress (Figure 7B). Following euthanasia, the heart was harvested and 12 circumferential transmural left ventricle samples (approximately 1g) were collected, weighed and dried for 24h in a 60°C (see Figure 6). Each tissue and blood sample was exposed to neutron beams and microsphere densities were measured in a gamma counter. Assuming that microspheres were uniformly mixed in the atrium and that complete entrapment of microspheres in the

heart's capillary bed occurred during the first circulation, MBF was calculated using the following equation (Ruel *et al.*, 2003b):

$$MBF(ml/\min/g) = \frac{withdrawal\ rate(ml/\min)}{weight\ tissue\ sample\ (g)} \times \frac{isotope\ counts(tissue\ sample)}{isotope\ counts(reference\ blood\ sample)}$$

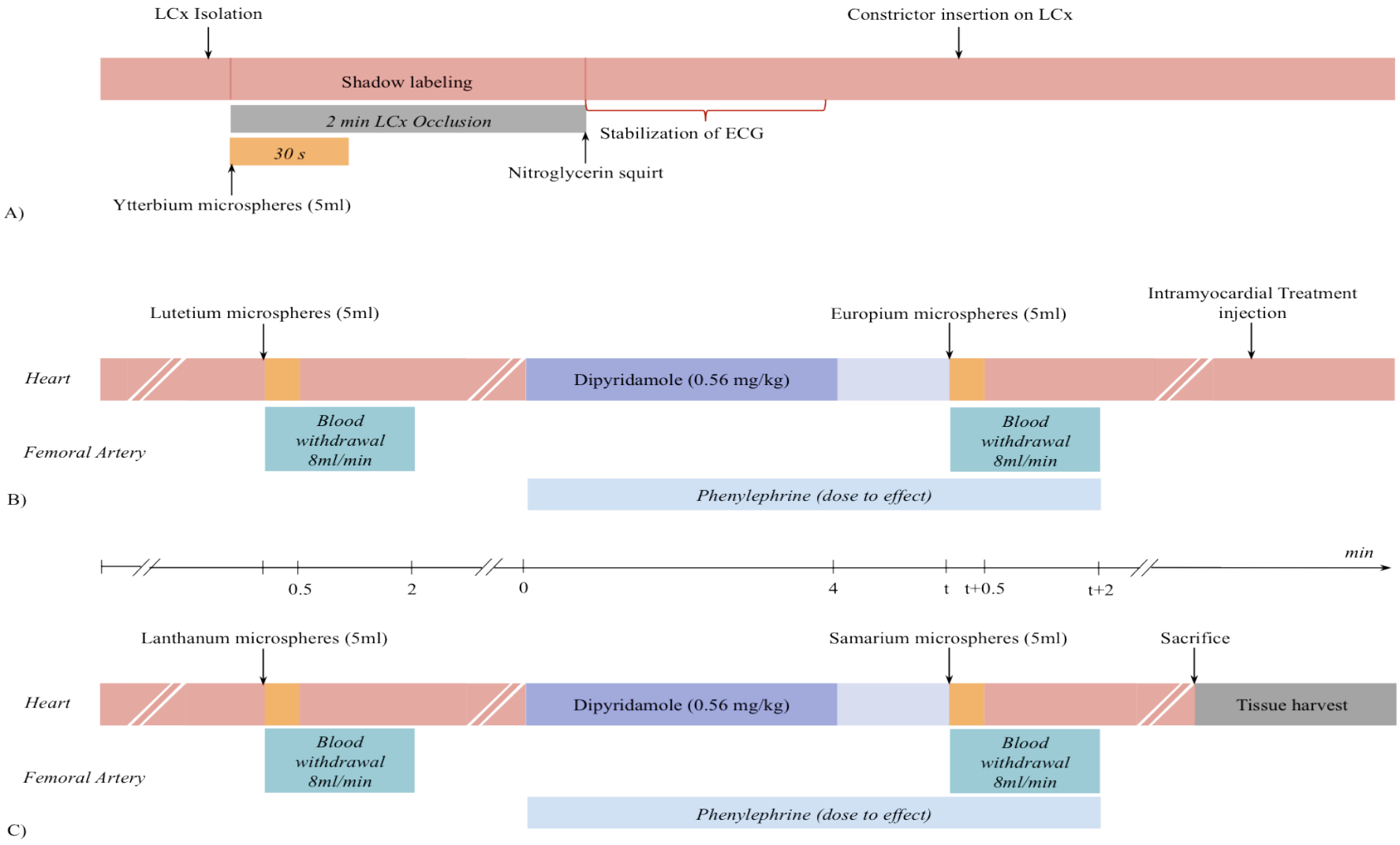

Figure 1: Microsphere protocol during surgery 1 (A), surgery 2 (B) and surgery 3 (C). The time line applies to surgeries 2 and 3.

1.1. Immunohistochemistry

Following euthanasia, sections from the LCx (LCx4) and the LAD territory were collected, fixed with 4% paraformaldehyde for 24h, dehydrated and paraffin embedded. The tissue was sliced in 6 μm thick sections. Immunohistochemistry against α-smooth muscle actin (SMA) was performed to identify arterioles. The primary α-SMA antibody (Abcam, Cambridge, USA) was and used in conjunction with texas red (Vector, Burlington, Canada). Six pictures per slides were taken and vessels were counted by 2-blinded examiners.

1.2. Investigation of constrictor occlusion

1.2.1. Computed coronary angiography

The feasibility of computed tomography angiography (CTA) was investigated in 2 animals. Pigs were prepared as per the normal protocol for PET scans and the animals were brought up to the PET/CT room properly anesthetised and under mechanical ventilation. The animals were placed on the PET/CT bed and appropriately positioned. Two scout CTs were first performed to locate the heart. To determine the optimal time to initiate the image acquisition, a timing bolus of contrast agent (Omnipaque 350, General Electric Healthcare, Mississauga, Canada) was injected at 4 ml/s (total of 40 ml) followed by a 20 ml saline flush at 4 ml/s. For CTA acquisition, 40 ml of contrast agent followed by 10 ml of saline were injected through an ear catheter at a rate of 4 ml/min, and a continual spiral scan was performed. Breath holds were simulated by turning the ventilator off for a period of 10 seconds. This was done for both scout CTs, the timing bolus scan and the actual image acquisition.

1.2.2. Ex-vivo CT scan

Ex-vivo analyses were performed on 5 ameroid constrictors. The outer metal ring was removed and the constrictors were placed on the NanoSPECT/CT (Bioscan, Washington, USA) camera bed in a "lying" position. Coronal, sagittal and transverse views were acquired. Images were reconstructed with InVivoScope 1.43 (Bioscan, Washington, USA) and visually observed to qualitatively determine if the vessel was completely occluded or not. A notch was made in the casein to differentiate each extremity of the constrictor.

1.2.3. Dissecting microscope

Ameroid constrictors deprived of the outer metal ring were observed under a dissecting microscope. Picture of each extremity of the vessel were taken and the vessel was qualitatively evaluated as "open" or "closed".

1.2.4. Haematoxylin and Eosin histology (H&E)

Following CT scan and visualisation under the dissecting microscope, the casein core of the ameroid constrictor was removed and the vessels were dehydrated, paraffin embedded and sliced for histology. Serial slicing was performed to examine the status of the vessel along its entire length. The three techniques used to investigate the occlusion of the constrictor were compared.

1.3. Statistical Analyses

Results are presented as mean ± standard error. Statistical analyses were performed with Sigma Stat (Ashburn, VA). Paired Student t-tests were used to compare values between the affected and remote regions of the heart, and between baseline and follow-up. Comparisons between groups were done using a one-way analysis of variance (ANOVA) and two-sample Student t-test assuming equal variances. Significance was reported for $p<0.05$.

3. RESULTS

A total of 25 animals survived and were used for analyses. In addition to those, 3 pigs died during the first surgery, 1 died at induction of the first anesthesia, 2 died at PET during the first stress scan, and 1 died during the second stress scan and 1 died while during a CTA. All remaining pigs completed the study protocol. Unless otherwise specified, reported findings are for the LCx territory.

3.1. Myocardial ischemia and hibernation in the ameroid constrictor model

Two and three weeks after ameroid placement, PET and microsphere analyses both showed a marked reduction in MBF at rest, MBF at stress, and MFR in the LCx territory, compared the left anterior descending (LAD) control region (Figure 1 and Table 2). Mean mismatch and match scores were higher in the LCx than in the LAD region (9.07±1.81 *vs.* 3.24±1.14; $p<0.001$ and 7.24±1.27 *vs.* 3.81±1.05; $p=0.002$, respectively). Twelve pigs had more mismatch than match (Mismatch: 11.89±2.60 *vs.* Match: 4.98±0.74; $p=0.014$), 6 out of the 18 had more match than mismatch (Mismatch: 4.78±0.96 *vs.* Match: 11.44±3.01; $p=0.041$). The three sham animals had no perfusion defect at baseline under rest conditions (LCx: 0.92 ±0.09 *vs.* LAD: 0.92±0.09 ml/min/g $p=0.95$) but showed higher stress MBF in the LAD compared to the LCx (LCx: 1.65±0.09 *vs.* LAD: 1.83±0.09 ml/min/g; $p=0.02$). However, MFR was not significantly different between the two territories (LCx: 1.84±0.25 *vs.* LCx: 1.97±0.19; $p=0.31$). Mismatch and match scores were low and did not differ between the two areas of the heart (Mismatch: LCx: 0.14±0.07 *vs.* LAD: 0.14±0.08; Match: LCx: 0.14±0.08 *vs.* LAD: 0.13±0.12).

	PET (n= 25)			Microspheres (n=20)		
	LCx	LAD	*p*-value	LCx	LAD	*p*-value
Rest	0.85 ± 0.04	0.95 ± 0.05	$p<0.001$	0.60 ± 0.07	0.72 ± 0.08	$p=0.01$
Stress	1.15 ± 0.10	1.51 ± 0.13	$p<0.001$	0.74 ± 0.09	1.46 ± 0.16	$p<0.001$
MFR	1.40 ± 0.11	1.62 ± 0.14	$p<0.001$	1.68 ± 0.27	2.42 ± 0.38	$p=0.02$

Table 2: Absolute myocardial blood flow (ml/min/g) 2 weeks (PET) and 3 weeks (microspheres) after ameroid placement on the proximal LCx.

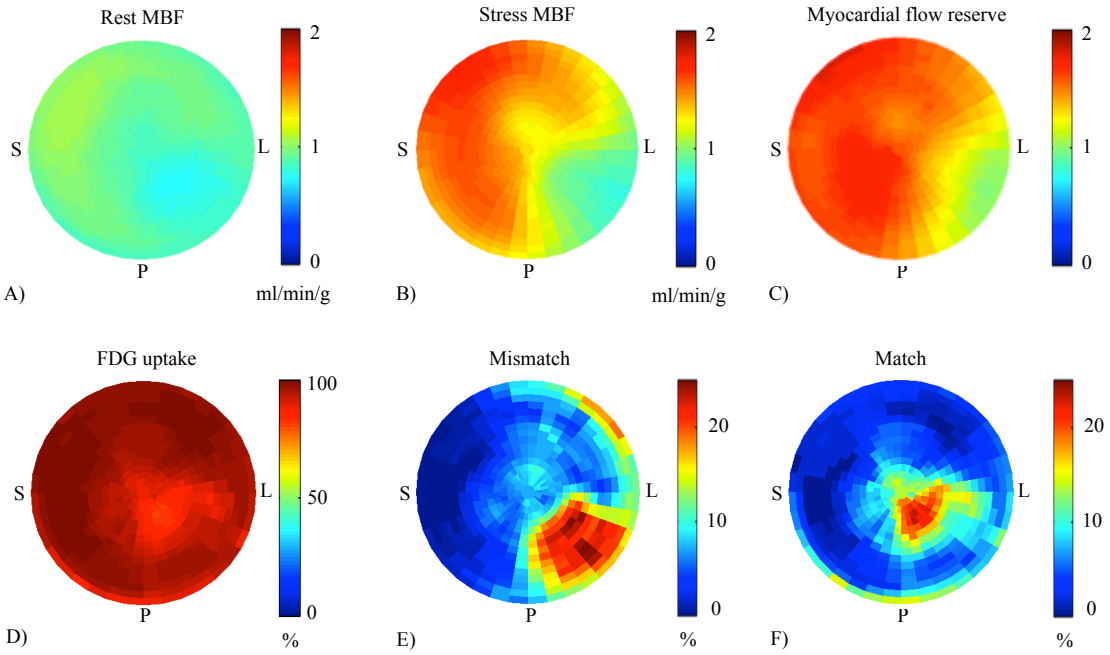

Figure 8: Myocardial ischemia and hibernation. Pooled averaged polar maps of all animals two weeks after ameroid placement on the LCx. Reduced resting MBF (A), reduced dipyridamole-induced stress MBF (B) and reduced MFR (C) were observed in the LCx territory compared to the LAD. Raw FDG uptake (D). Segments with maintained FDG uptake and reduced perfusion correspond to mismatch- hibernation (E), while segments with a matched reduction in perfusion and viability represent scar (F).

All animals instrumented with a constrictor except for 1 had at least 1 abnormal segment on echocardiography. The mean WMSI was 1.25 ± 0.04 and all abnormalities were located in the 6 segments representing the lateral, inferior and posterior walls. The mean LVEF was 56.39±1.43. The mean LVEF of the 3 sham animals was 62±1.53.

3.2. Effect of CAC transplantation on MBF measured by PET

At baseline, there was no difference between groups in rest MBF (p=0.92), stress MBF (p=0.60) and MFR (p=0.33). Three weeks after treatment, rest MBF remained unchanged in all groups (Figure 9A), while stress MBF increased in the cells+matrix group only (0.74±0.12 to 1.09±0.11 ml/min/g; p=0.007) (Figure 9B). Similarly, MFR did not change in the control and cells groups (p=0.87 and p=0.86 respectively), while it significantly improved when cells were delivered within the matrix (from 0.91±0.1 to 1.39±0.13; p=0.01) (Figure 9C).

Changes in stress MBF varied between groups (p=0.04). The highest increase was in the cells+matrix group (+75.61±39.18%), which was significantly higher than PBS and cells (+4.61±7.65%; p=0.01). Likewise, the increase in MFR was greatest in the cells+matrix group (+68.53±30.46%), compared to PBS and cells (+7.55±10.54%; p=0.02).

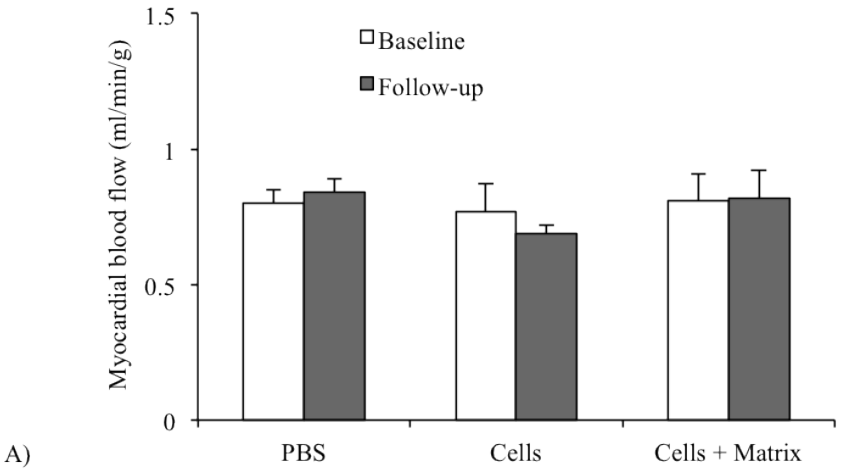

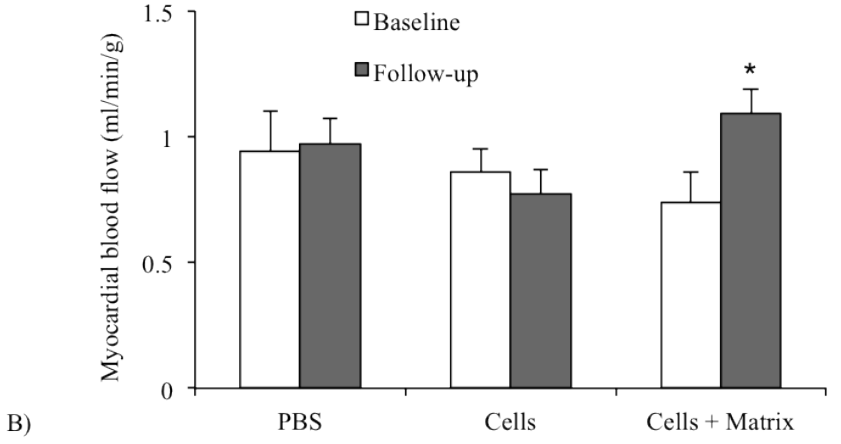

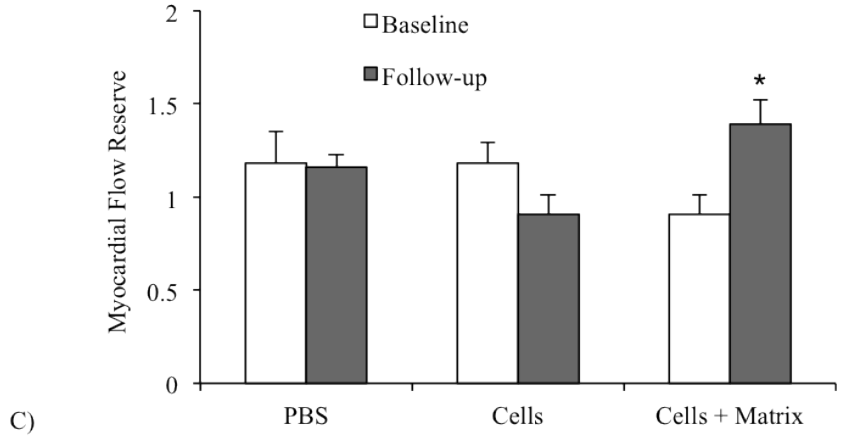

Figure 9: Effects of CAC delivery on regional MBF measured by PET. Rest MBF (A), stress MBF (B) and MFR (C) in the affected region at baseline and follow up. Stress MBF and MFR were only improved when cells were delivered within the collagen matrix; *$p<0.05$.

3.3. Effect of CAC transplantation on MBF measured by microspheres

When comparing groups, only 17 pigs had baseline and follow-up measurements and were included in the analysis. Technical errors such as microsphere injection outside of the atrium or wrong rate of blood withdrawal are responsible for the incomplete dataset.

There was no difference in rest MBF (p=0.42), stress MBF (p=0.84) and MFR (p=0.78) between groups at baseline. Under resting conditions, MBF remained unchanged in all treatment groups between baseline and follow-up (Figure 10A). Stress MBF increased from 0.84 to 2.18 ml/min/g (p=0.008) in the cells+matrix group, but did not change in a statistically significant manner in PBS (p=0.09) and cells (p=0.06*)* groups. At follow-up, stress MBF was significantly higher in the cells+matrix group compared to controls (2.18±0.35 *vs.* 1.09±0.1 ml/min/g; p=0.01) and cells (2.18±0.35 *vs.* 1.15±0.23 ml/min/g; p=0.03). There was no difference between controls and cells (p=0.84) (Figure 10B). MFR did not significantly improve in any of the groups; however, there is a trend towards the highest increase in the cells+matrix group (Figure 10C).

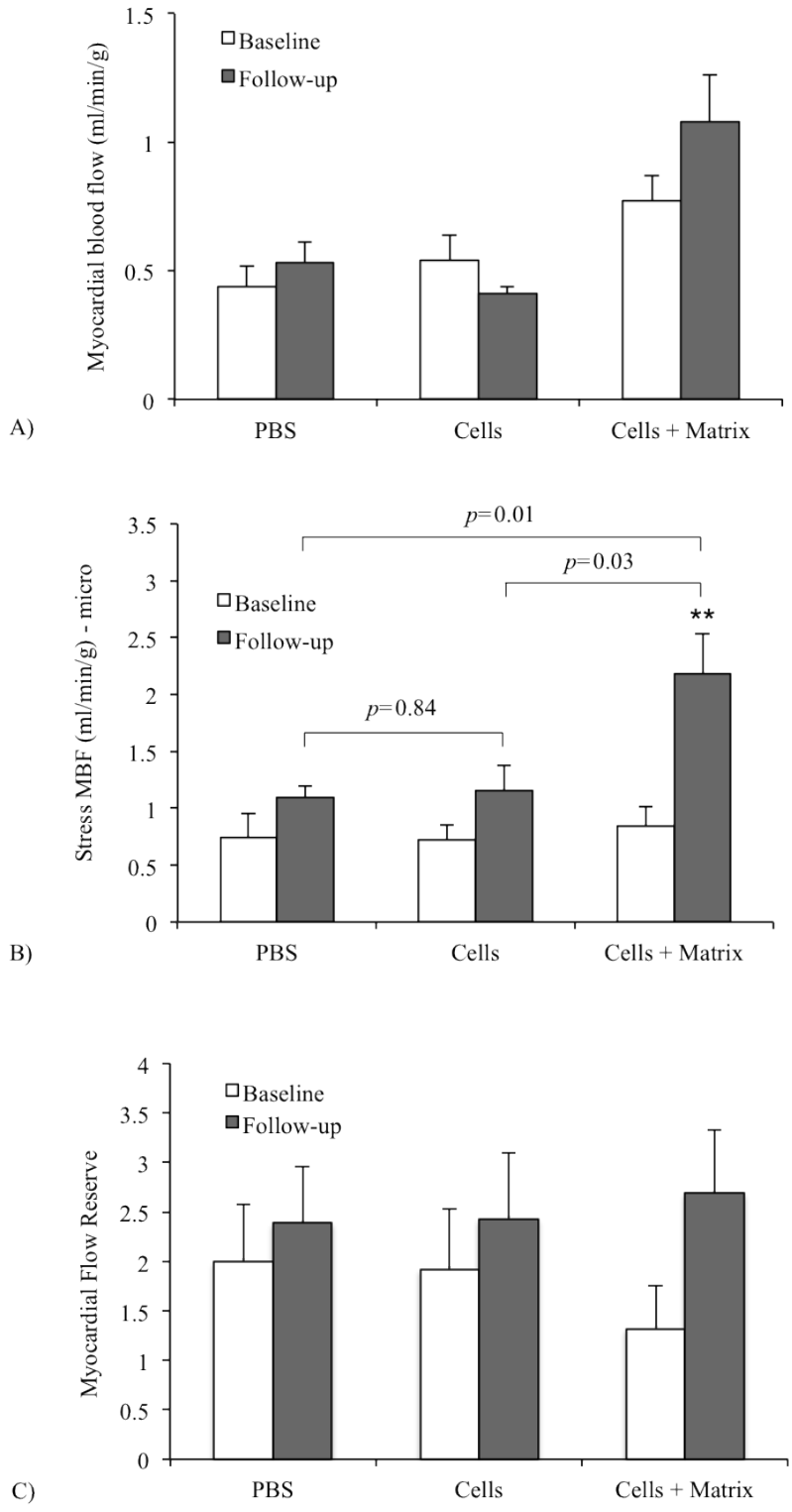

Figure 10: Effects of CAC delivery on regional MBF measured by microspheres. Rest MBF (A), stress MBF (B) and MFR (C) in the affected region at baseline and follow up. Stress MBF was improved only in the cells+matrix group and was higher at follow-up compared to the cells and to the PBS groups. There was no difference in follow-up MBF between the cells and the PBS group; **p≤0.01 *vs.* baseline

3.4. Effect of CAC transplantation on myocardial viability measured by PET

Mismatch (p=0.88) and match scores (p=0.26) did not differ between groups at baseline. Three weeks after treatment, mismatch scores were significantly lower in every treatment group compared to baseline (Figure 11A). Match scores were significantly decreased only in the cells+matrix group (p=0.007) (Figure 11B). In the control group, 2 pigs had a global reduction in mismatch paralleled by a global increase in match, suggesting progression from viable to scar tissue. At follow-up, mean mismatch scores were lower in the cells+matrix and cells groups compared to controls (respectively 0.19±0.09 *vs.* 9.38±2.73, p=0.02; 1.06±0.7 *vs.* 9.38±2.73, p=0.04).

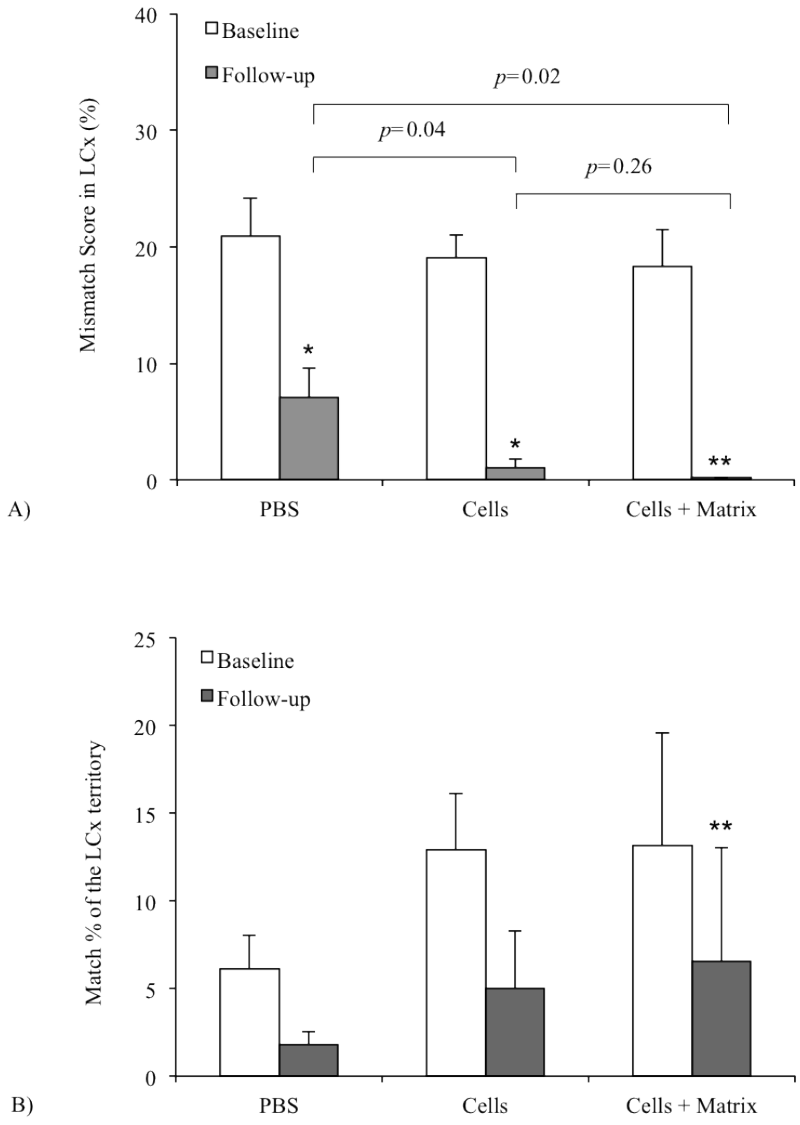

Figure 11: Effects of CAC delivery on myocardial viability. Mismatch was significantly reduced in all treatment groups; the most significant decrease occurred in the cells+matrix group. There was no difference between groups at baseline (p=0.88). At follow-up, mismatch was reduced in the cells and in the cells+matrix groups compared to baseline (A). Match was significantly reduced only in the cells+matrix group (B); *p≤0.05 *vs.* baseline; **p≤0.01 *vs.* baseline.

3.5. Effect of CAC transplantation on LV function measured by echo

From baseline LVEF, the cells+matrix group trended to show an increase in LVEF (+12.0±6.7%, p=0.06), which was not observed in PBS and cells alone groups (−0.10±2.81%) (Figure 12). Regional wall motion of the dysfunctional segments improved when cells were delivered within the matrix (p<0.05), but not in the cells alone (p=0.10) or PBS groups (p=0.2).

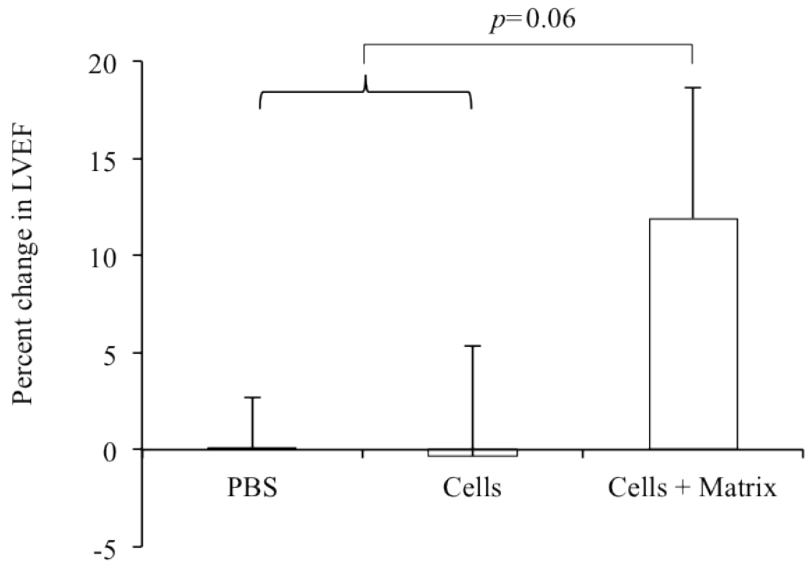

Figure 12: Effects of CAC delivery on LVEF. A trend towards an improvement in the cells+matrix group is observable.

3.6. Effect of CAC transplantation on arteriole density

Cells+matrix treated hearts demonstrated greater arteriole number (10.86±1.27 arterioles/field of view) in the LCx territory compared to cells-treated animals (6.28±0.92; p=0.01) and controls (4.25±0.64; p<0.001). Mean arteriole number did not differ between cells and PBS treated animals (p=0.08) (Figure 13). There was a strong positive correlation between follow-up microsphere MBF at stress and the number of arterioles in the LCx (r=0.7; p=0.008) and LAD (r=0.66; p=0.01) territories.

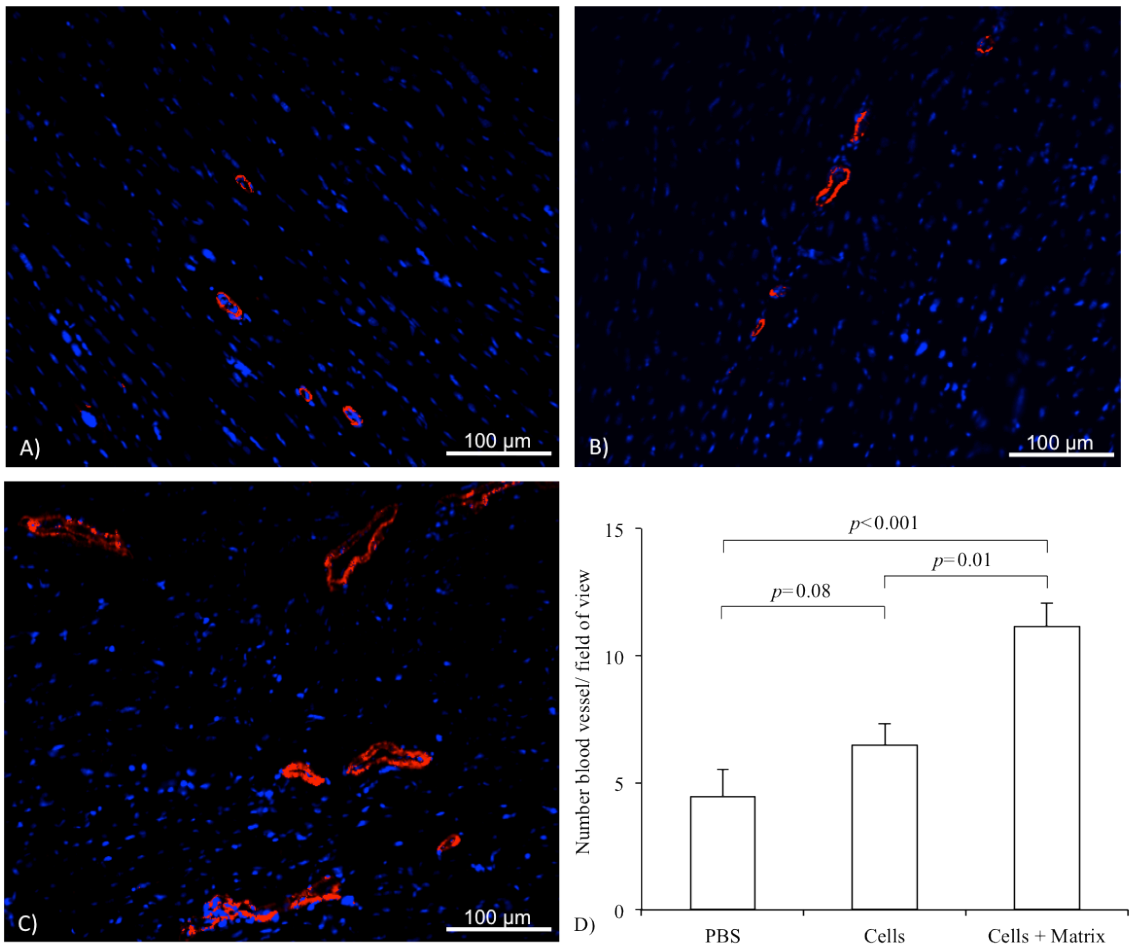

Figure 13: Effect of CAC transplantation on arteriole number at follow-up. Representative images of arteriole numbers in control (A), cells (B) and cells+matrix groups (C). Arteriole number was > 50% higher in the cells+matrix group compared to controls (D).

3.7. Constrictor imaging

CT images of the ameroid constrictor were clear and distinction between the casein core, the vessel wall and the vessel lumen was possible (Figure 14). Following qualitative analyses of the images, only 3/5 vessels appeared closed at one location along the length of the constrictor. The distinction between the casein core, the vessel wall and the vessel lumen was also clear in the pictures taken with the dissecting microscope (Figure 15 A & B). On H&E sections, the vessel walls, thrombi and collagen accumulation were clearly visible. A thrombus was observed in every vessel. Physical narrowing of the lumen was only visible in 3/5 animals (Figure 15 C & D), and these animals corresponded to the ones where the vessel appeared closed on CT images. Whether it was by physical narrowing of the lumen or formation of a thrombus, all vessels appeared closed after 7 weeks.

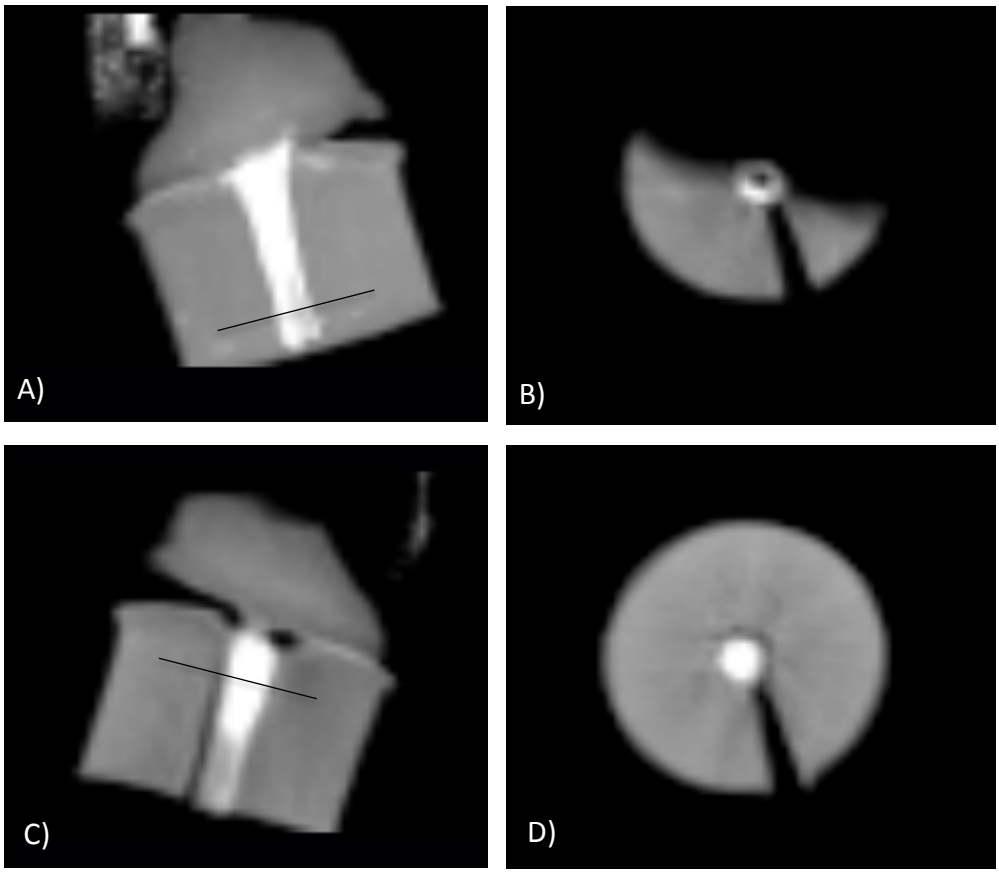

Figure 14: *Ex-vivo* CT evaluation of the ameroid constrictor. Images (A) and (B) are sagittal views of the ameroid constrictor. (B) and (D) are cross section images taken at the level of the line in the corresponding sagittal views. The vessel appears open in (B) whereas obstruction of the vessel is apparent in (D)

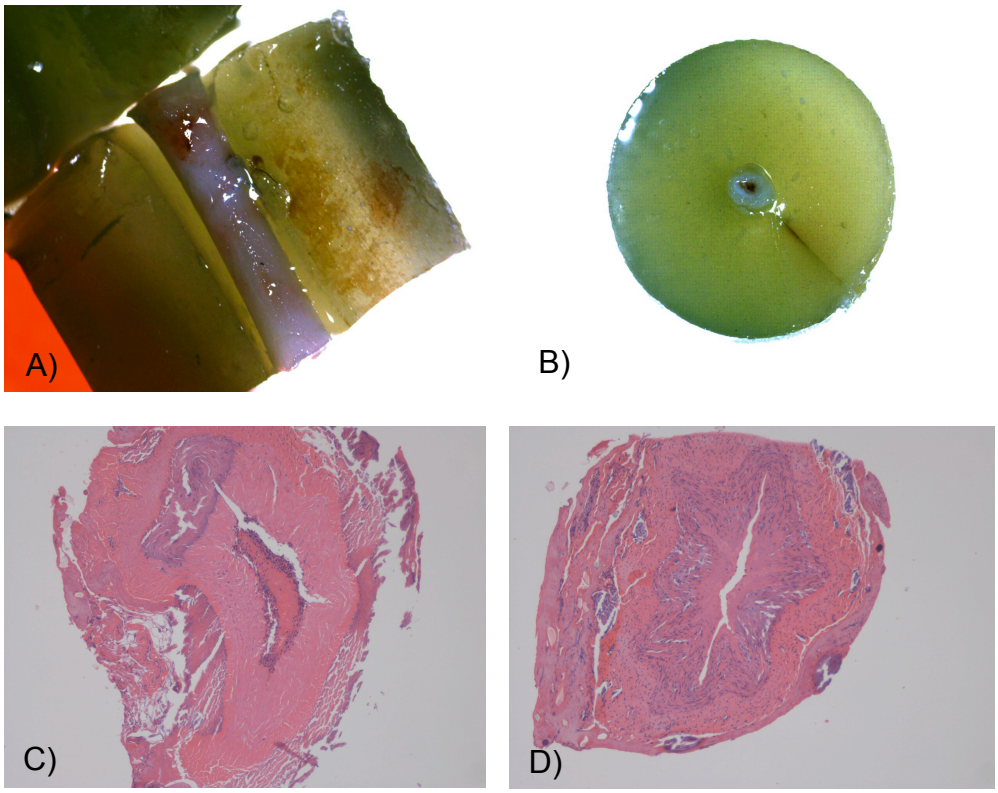

Figure 15: *Ex-vivo* evaluation of the ameroid constrictor. Images (A) and (B) were taken using a dissecting microscope. A longitudinal view of the vessel is shown in (A) and image (B) clearly shows the presence of a thrombus in the lumen. Pictures (C) and (D) are H&E stains of the LCx, 7 weeks after implantation around the artery. Mechanical compression of the vessel wall is clearly observed. A thrombus obstructing the vessel is visible in (C).

4. DISCUSSION

In this study, we first induced and characterised a model of chronic myocardial ischemia and hibernation and subsequently used it to evaluate the benefit of CAC delivery on myocardial ischemia and hibernation.

4.1. Ameroid constrictor model of chronic myocardial hibernation

The first part of this study was to characterise the ameroid constrictor model of myocardial ischemia/hibernation with PET. To evaluate the effect of the ameroid constrictor on the LCx, this region was systematically compared to the non-affected (remote) LAD region. After 2 and 3 weeks of ameroid placement, there was a marked reduction in rest MBF in the affected region, which was more pronounced under stress condition, leading to an impaired MFR. The ameroid constrictor model has been extensively used to study the development of collaterals following a vessel occlusion. Reduced MBF at rest was also previously observed in the LCx endocardium after 3 weeks (Roth *et al.*, 1987; White *et al.*, 1992) whereas other studies reported no difference between the 2 regions at 20 (Shen *et al.*, 1996) and 26 days (Radke *et al.*, 2006) respectively. These studies however reconcile as stress MBF and MFR are consistently diminished in the stenosed area compared to the control region (O'Konski *et al.*, 1987; Roth *et al.*, 1987; Roth *et al.*, 1990; Radke *et al.*, 2006). These findings were corroborated with our observations. In addition to myocardial ischemia, this model successfully demonstrated myocardial hibernation in a majority of animals and mismatch was predominantly present in the LCx territory, as expected. Hibernation was previously detected by dobutamine stress echocardiography (Almeda *et al.*, 2004; Schneider *et al.*, 2007; Schneider *et al.*, 2008) or NOGA LV electromechanical mapping (Kamihata *et al.*,

2002) in this model, but we are the first ones to use PET in this setting. In contrast to dobutamine stress echocardiography that detects the contractile reserve of the heart (Wu & Lima, 2003; McLean *et al.*, 2009), PET detects viability at the cellular level and shows higher sensitivity for detection of viable segments (Schinkel *et al.*, 2007). Using this technique we also detected myocardial scar, which corresponds to regions with reduced perfusion and a matched reduction in viability. Previous studies have also reported scaring, ranging from ~ 0 to 37% of the area at risk but these observations were limited to histological assessments (O'Konski *et al.*, 1987; Roth *et al.*, 1987; White *et al.*, 1992; Almeda *et al.*, 2004). Our PET scan data showed that the segments with reduced viability were adjacent to segments with maintained viability, which is consistent with the belief that hibernating myocardium is composed of normal, stunned, hibernating and scarred tissue (Hughes *et al.*, 2001). One third of our animals had more match than mismatch; one possible explanation is that the closure of the constrictor is in fact not a gradual process. Although not specific to coronary artery constrictors, some researchers have noted that occlusion of the vessel can precede physical closure of the constrictor's lumen. When implanted in the peritoneal cavity of rats, the inner diameter of constrictors was reduced by only 32% after 6 weeks (Adin *et al.*, 2004). This suggested that physiological processes, such as thrombosis, rather than swelling of the hygroscopic material, are likely responsible for vessel occlusion. In addition to causing external compression of the vessel, ameroid constrictors also cause mechanical trauma that may lead to endothelial damage, platelet aggregation and thrombus formation, which in turn may result in inflammation and local fibrosis (Unger, 2001; Besancon *et al.*, 2004), obstructing blood flow before physical closure of the vessel. In our case, some vessels had a reduced

diameter, whereas others did not. A thrombus with or without local fibrosis was however observed in every vessel analysed. When comparing histological and CT images, we noted that the vessels appearing closed on CT images corresponded to vessels with a smaller lumen on histology. On the other hand, vessels appearing open on CT images corresponded to vessels with un-compressed vessel walls but with luminal thrombus. This suggests that *ex-vivo* CT is not an ideal technique to determine the status of the vessel closure. An alternate solution could be an *ex-vivo* CT scan using contrast agents such as the ones used in CTAs. If the vessel were patent, dye would be observed distally, whereas no contrast would appear on CT images if the vessel were obstructed. We considered this technique but were unable to dissect a segment of artery proximal to the device, preventing successful injection of contrast agent.

Echocardiography results showed the presence of wall motion abnormalities two weeks following constrictor implementation. These abnormalities were located in the inferior, posterior and lateral walls, with the most affected segments being in the posterior wall. No absolute correlation between the segments with impaired MBF and function was established in this study. The lack of standardisation between imaging modalities complicates the task of accurate inter-modality comparisons. Although PET and echocardiography are both used to image the LV, these modalities have evolved separately with respect to the orientation of the heart, the number and nomenclature of segments, and the attribution of segments to coronary arteries (Cerqueira *et al.*, 2002). Previous work using either electromechanical mapping (Fuchs & Kornowski, 2005; Tuzun *et al.*, 2009) or 2D strain and contrast echocardiography (Caillaud *et al.*, 2010) reported correspondence between areas of reduced perfusion and reduced mechanical as

well as electrical function (Fuchs & Kornowski, 2005). Because no baseline echocardiography was done due to the already extensive protocol, it is difficult to evaluate whether there was a reduction in LVEF or FS. However, compared to sham animals that did not undergo ameroid constrictor placement, the mean LVEF and FS was reduced in instrumented animals, suggesting an impaired function after 2 weeks. In the literature, pre-constrictor LVEFs range from 65 to 69% and post-constrictor (4 weeks) LVEFs range from 33 to 46% (Ninomiya *et al.*, 2003; Chen *et al.*, 2009a), which is in agreement with our values.

One limitation of this model is the irregular closure rate of the ameroid constrictor. Some studies report complete vessel occlusion after a period of 2 (Schneider *et al.*, 2007; Schneider *et al.*, 2008; Krause *et al.*, 2009; Schneider *et al.*, 2009) or 4 (Fuchs & Kornowski, 2005; Robich *et al.*, 2010) weeks, whereas others report 10/14 and 3/22 constrictors occluded after 2-3 (Johnson *et al.*, 2008) and 4 weeks (Chen *et al.*, 2009b) respectively. This variability may come from inaccurate evaluation of the constrictor's size leading to an imperfect fit of the device around the vessel, or inter-animal variation in the growth of the artery and local inflammatory response (Caillaud *et al.*, 2010). Tuzun *et al*. (Tuzun *et al.*, 2009) reported that after 30 days, the initial internal diameter of the ameroid constrictor (2.25-2.75 mm) did not affect the size of the ischemic area (NOGA) or coronary flow (TIMI grades). The degree of ischemia however depends on the general coronary anatomy and the initial amount of collaterals, the location of the constrictor on the artery (proximal or distal) and relative to side branches, the animal's level of activity (Unger, 2001) and the animal's inflammatory response to the ameroid constrictor (Sereda & Adin, 2005). Because adding coronary angiography to our protocol

was technically impossible, we investigated different *in-vivo* and *ex-vivo* techniques to determine the status of the ameroid constrictor. By opposition to conventional coronary angiography, CT angiography is a non-invasive procedure that necessitates only a peripheral intravenous access. In humans, optimal image quality is obtained when heart rate is reduced below 63 bpm (Husmann *et al.*, 2011), but 65 bpm appears to be sufficient in pigs (Kumar *et al.*, 2007; Shetty *et al.*, 2008). In our animals, heart rates were 120 bpm and 110 bpm at the time of the scan, and administration of Metoprolol did not reduce heart rate. Nevertheless, the procedure was well tolerated by the first practice animal; images were of good quality and the artefact created by the outer metal ring of the ameroid constrictor did not prevent accurate evaluation of the coronary occlusion status. Unfortunately, the second pig did not tolerate this procedure and died during the CTA. To prevent any further deaths, it was decided not to pursue with CT angiography. As discussed above, the status of the constrictor was evaluated in 5 animals *ex vivo* and showed occlusion of the vessel in all cases. Although these results were encouraging and suggested a similar pattern in all animals, this investigation was performed at the end of the study rather than at the time of treatment injection, and only a subset of animals were tested. In this regard, the randomised blinded design of this study added considerable strength to the investigation. Randomisation was used to attribute by chance rather than by choice a treatment/control group to each animal. This process minimised the risks of biased treatment attribution and increased the chances of separating the population in comparable groups. For instance, while the status of the ameroid constrictor was unknown at the time of treatment administration, randomisation likely distributed all animals, regardless of the constrictor status, in similar ratios between groups, minimising

potential bias and variability between groups. Another strong point of this study is its blinded aspect. Every set of results for each animal was analysed in a blinded fashion and groups were revealed only upon completion of all analyses. This prevented bias while analysing the data and increased the power of this study significantly.

4.2. Delivery of CACs and matrix benefits

This study is the first to demonstrate, in a preclinical model of hibernating myocardium, that the vasculogenic potential of transplanted CACs is greatly enhanced when cells are delivered in a biomaterial. In our opinion, this is important since myocardial hibernation is present in up to 50% of CAD patients (Schinkel *et al.*, 2007) and over 1/3 of these may not get appropriate treatment (Beanlands *et al.*, 1998). Consequently, the applicability of cell-based therapies is particularly relevant in this population, as early cell and biomaterial delivery may promote revascularization before irreversible damage to the myocardium occurs, in a context where currently available therapies are commonly not feasible.

The combination of autologous angiogenic cells and naturally occurring extracellular matrix components successfully improved stress MBF and MFR in our study. Improved MFR suggests an increased response capacity to higher oxygen demands by recruitment or generation of new vasculature. Histological findings were also supportive of the enhanced benefits conferred by the matrix, as cell delivery in a matrix doubled the number of arterioles in the myocardium. These animals also displayed lower amounts of mismatch and match, suggesting a better recovery of myocardial viability following matrix delivery of CACs. This was paralleled with an improvement in wall motion and a strong trend towards an improvement in LVEF, despite the relatively small

area of hibernation, the early follow-up time-points, and the physiological and metabolic rather than functional emphasis of the experiments. Enhanced vasculogenesis was also noted and, in the presence of hibernating myocardium, may constitute an important mechanism of improved LV function in animals or patients undergoing successful cell therapy.

Notably, the transplantation of cells alone was not successful in increasing MBF or reducing match scores. CACs play an endogenous role in tissue regeneration, and their contribution as transplanted agents has been established in small animal models of ischemia. Only two populations of progenitor cells from the PB have been used in large animals models of chronic ischemia. Non-adherent CD31+ cells improved Rentrop scores and capillary density, reduced the area of ischemia and improved LVEF. In our case, transplantation of CACs alone did not improve MBF or LV function. Similar results were found in another study using CACs, where only cells transduced to express FGF-1 reduced the perfusion defect. We harvested blood 2 weeks following the insertion of the ameroid constrictor; at this time, myocardial ischemia was well established in all animals and myocardial hibernation was present in a majority of them, possibly impairing their function as it was observed in patients with CAD (Vasa *et al.*, 2001). Cell viability is rarely reported in the literature, but one group using freshly isolated bone-marrow derived mononuclear cells reported a viability >95% (Tse *et al.*, 2003), and another one reported a 70% viability of frozen mesenchymal stem cells the time of injection (Silva *et al.*, 2005). In our case, cell viability averaged 84% and was similar between the two groups. Similarly, we injected on average 33 million cells, which is well within the range found in the literature (Kamihata *et al.*, 2002; Chen *et al.*, 2009b), although this dose

might be insufficient to observe benefits in this setting. A dosing study by Silva *et al.* (Silva *et al.*, 2011) showed a trend towards higher capillary density with increased cell dose, and they also demonstrated that the local number of cells rather than the total number injected was a better predictor of increased capillary density and reduced fibrosis: when segments were injected with over 20 million cells, they had the highest capillary density and the lowest amount of fibrotic tissue. Considering that we injected a total of 33 million cells in 12 different locations, it is possible that the local cell number was sub-optimal to lead to increased vasculogenesis. In addition, it is well recognised that only small numbers of transplanted cells survive in the host tissue, which limits their effects. When delivered directly into the myocardium, retention rates vary between 1 and 11% (Hou *et al.*, 2005). Although much higher than systemic or intracoronary delivery (3-5% retention rates (Hou *et al.*, 2005; Penicka *et al.*, 2005)), the number of cells retained in the target area remains low with this technique. In this regard, our collagen-based matrix can improve cell retention and prevent excessive relocation of transplanted cells to non-target tissues, (Zhang *et al.*, 2008) and improve capillary density (Suuronen *et al.*, 2006b).

Collagen is a ubiquitous molecule of the ECM that is adhesive to many cell types. Its structure allows for integration of CACs within its pores, thereby increasing their retention. As discussed above, collagen can be formed into thermosensitive hydrogels used for cell delivery. Upon their delivery, hydrogels can take the shape of the tissue before solidifying and entrapping cells. Collagen-based matrices can also be used as a 3D environment for *in-vitro* cell culture. Recent work from our lab has demonstrated that the culture of CACs on a collagen-based matrix can enhance their function (Kuraitis *et al.*,

2011). First, these cells showed greater survival upon exposure to hypoxia. The PI3K/Akt pathway is known to increase resistance to apoptosis (Dai *et al.*, 2008), and increased p-Akt concentrations were observed in the cells cultured on the collagen matrix. This demonstrated increased activation of survival pathways, which correlated with increased survival in hypoxic conditions. In addition, the activation of the Akt pathway was shown to increase transendothelial migration of CACs (Hur *et al.*, 2007). Greater migratory potential into basal membrane in response to chemotactic stimulus was also observed in cells cultured on the matrix, as well as greater *in-vitro* contribution to capillary-like structures when co-cultured with ECs. Although in our study CACs were cultured on fibronectin and only delivered with the collagen matrix as a vehicle, these results might provide insights into the mechanisms leading to the greater contribution to regeneration. It is possible that interaction of CACs cultured on fibronectin with the collagen matrix leads to similar changes in CACs, preventing apoptosis of the cells when exposed to the ischemic environment of the damaged heart, increasing migration of cells towards the heart's extracellular matrix and increasing their contribution to the formation of new capillaries.

The exact mechanisms explaining the benefits conferred by transplantation of therapeutic cells remains to be confirmed. Mounting evidence suggests a paracrine contribution of the transplanted cells, secreting pro-angiogenic factors as well as contributing to an up-regulation of host derived cytokine secretion. The increased retention and viability of cells when delivered via the collagen matrix may provide prolonged paracrine effects. In addition, collagen itself is a highly adhesive molecule to many cell types, and its injection alone was shown to improve LVEF in infarcted rat

myocardium (Dai *et al.*, 2009). When injected into the ischemic hindlimb of rats, vascularisation of the matrix was observed with and with out cells, suggesting inherent properties of the matrix to promote revascularisation (Suuronen *et al.*, 2006b). In addition, biomaterials can be enhanced by incorporating adhesion molecules (Suuronen *et al.*, 2009) or coupled with delivery of growth factors, which were also shown increase vascular regeneration.

4.3. Microsphere *vs.* PET measurements

In this study, we used two different techniques to evaluate absolute MBF: PET and ILM. We have shown that microsphere and PET data behaved similarly although no direct correlation was reported. Excellent relationship between the two techniques was not expected, but a closer association could have been hoped for. In our study, MBF measured by microspheres was systematically lower that MBF measured by PET. At baseline both techniques showed a similar decrease in rest and stress MBF and MFR. Resting flow values measured by microspheres were within ranges found in the literature 2 weeks after constrictor placement (0.44 ml/min/g to 0.79 ml/min/g (Sato *et al.*, 2001; Ruel *et al.*, 2003a; Ruel *et al.*, 2003b; Boodhwani *et al.*, 2006; Boodhwani *et al.*, 2008a; Boodhwani *et al.*, 2008b)). When comparing follow-up results divided by groups, PET and microsphere data behave similarly. Under stress conditions, both techniques showed the highest MBF increase in the cells+matrix group. MFR was significantly increased in the cells+matrix group using PET but not microspheres; however, a trend towards the highest increase in the cells+matrix group was observed with microspheres.

A number of reasons can explain these differences in absolute MBF. First, microspheres were injected into the atrium over 30 seconds, while a reference blood

sample was simultaneously drawn from the femoral artery branch. Because the injection of microspheres was done manually, timing or rates of injection varied. In addition, if microspheres are not properly mixed in the atrium before travelling to the tissue or are not completely extracted on their first circulation, inaccurate measurements can be obtained (Heymann *et al.*, 1977). The second limitation involves the protocol used to slice the heart and collect samples for measurements. As described in the materials and method section, samples were collected from only 2 cross-sectional slices, which were further divided in 6 segments, completely omitting the septum. Twelve sections were therefore considered for analysis, but only 1 gram of tissue out of each section was used for microsphere counts. The counts obtained in each gram might not reflect MBF in the adjacent regions. In one animal, the entire LV (total of 40 segments) was used for analysis. A better correspondence between PET and microsphere MBF was obtained using this protocol. Although the absolute values remained different, the general pattern of MBF matched (Figure 16). The third limitation is the study design. PET and microsphere measurements were done one week apart because of technical reasons. In a more ideal protocol, microsphere and PET measurements would be done simultaneously, thereby minimizing metabolic variations due to the fasting state, the anaesthetic dose, the total amount of time under anaesthesia etc. Finally inadequate myocardial sampling or poor fit of the MBF quantification model can introduce variability in the PET data.

While detailed comparisons of absolute microsphere and PET MBF were beyond the initial scope of this study, both modalities confirmed the establishment of myocardial ischemia after two weeks and supported the enhanced benefits of cell delivery within the

matrix. In addition, a strong positive correlation between stress MBF and arteriole density validated those findings.

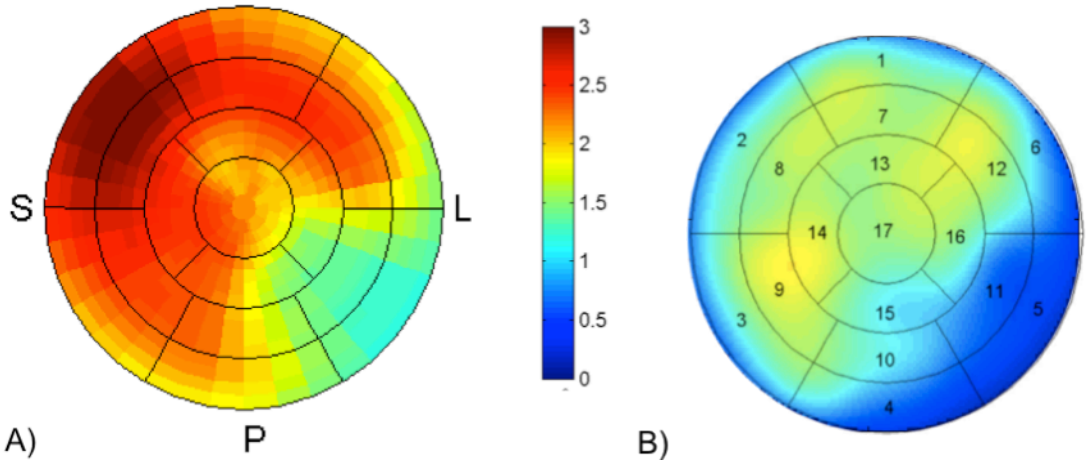

Figure 16: Absolute myocardial blood flow measured by PET (A) and microspheres (B). A better correspondence between PET and microsphere segments was obtained when samples from the entire heart (by opposition to 12 segments) were harvested and counted for microspheres.

4.4. Cell delivery technique

In our study, cells were delivered intramyocardially during the second thoracotomy. Clinically, direct intramyocardial cell injections were done during CABG when the heart was exposed; however, the majority of early studies delivered cells intracoronarily because this technique is less invasive. Newer techniques such as NOGA can evaluate ischemia, and allows for directed catheter-based transendocardial delivery of cells. This approach has been used in large animals studies (Kawamoto *et al.*, 2003; Schneider *et al.*, 2008; Schneider *et al.*, 2009) and in small clinical trials (Losordo *et al.*, 2007; Tse *et al.*, 2007; van Ramshorst *et al.*, 2009; Pokushalov *et al.*, 2010). In line with the higher cell retention rates when delivered intramyocardially, a recent meta-analysis demonstrated that LVEF was improved by 8.4% when BM progenitor cells were delivered directly to the myocardium (Wen *et al.*, 2011). A previous meta-analysis, including mainly studies where cells were delivered to the coronaries reported only a 3.4% improvement in LVEF (Abdel-Latif *et al.*, 2007). Although it is hard to compare both meta-analyses, this suggests that intramyocardial delivery of cells is the method of choice and that progress was made in progenitor cell therapy.

4.5. Limitations

One main limitation of this study is the absence of a collagen only group. As collagen can have positive effects on LV function when delivered alone (Dai *et al.*, 2009), the addition of this group would have provided an additional control for our data. In addition, as discussed previously, no angiography was performed to evaluate the status of the LCx at the time of cell injection. Although the randomised attribution of treatment likely reduced bias between groups, information on the status of the constrictors would

have permitted to exclude animals with non-occluded vessel, or would have provided an additional parameter to control for this in the analyses. Given this limitation, the observation that the cell + matrix group was superior to the other treatments may actually be an underestimation of its true potential to restore perfusion and function to the heart. A new model was recently developed and consists of the insertion of the constrictor around the LCx, and subsequent ligation of the artery downstream of the constrictor after 2 weeks (Ikonen *et al.*, 2007; Patila *et al.*, 2009). This approach standardises lesion size and may be an option for new large animal studies. Finally, the difference in the number of cells injected between the two groups might appear as a limitation to this study; however, although the mean numbers diverge, this difference is not significant ($p=0.62$).

5. CONCLUSION

This study demonstrated successful development of myocardial hibernation using the well-established ameroid constrictor model of chronic ischemia. This study was also the first to demonstrate that delivering CACs within a collagen matrix can improve MBF, reduce the extent of hibernation, and reduce wall motion abnormalities to a greater extent than cells alone. These results obtained in a preclinical model and in blinded fashion confirm previous small animal work, and constitute an important step towards the application of collagen matrices to support cell therapy and treat myocardial hibernation in the clinical setting.

REFERENCES

Abdel-Latif A, Bolli R, Tleyjeh IM, Montori VM, Perin EC, Hornung CA, Zuba-Surma EK, Al-Mallah M & Dawn B. (2007). Adult bone marrow-derived cells for cardiac repair: a systematic review and meta-analysis. *Arch Intern Med* **167,** 989-997.

Adin CA, Gregory CR, Kyles AE, Griffey SM & Kendall L. (2004). Effect of petrolatum coating on the rate of occlusion of ameroid constrictors in the peritoneal cavity. *Vet Surg* **33,** 11-16.

AHA. Heart Disease & Stroke Statistics - 2010 Update. American Heart Association, Dallas, Texas.

Ali Raza J, Reeves WC & Movahed A. (2001). Pharmacological stress agents for evaluation of ischemic heart disease. *Int J Cardiol* **81,** 157-167.

Allman KC, Shaw LJ, Hachamovitch R & Udelson JE. (2002). Myocardial viability testing and impact of revascularization on prognosis in patients with coronary artery disease and left ventricular dysfunction: a meta-analysis. *J Am Coll Cardiol* **39,** 1151-1158.

Almeda FQ, Glock D, Sandelski J, Ibrahim O, Macioch JE, Allen T, Dainauskas JR, Parrillo JE, Snell RJ & Schaer GL. (2004). The effect of percutaneous transmyocardial laser revascularization on left ventricular function in a porcine model of hibernating myocardium: a pilot study. *Cardiovasc Radiat Med* **5,** 132-135.

Angelini A, Maiolino G, La Canna G, Ceconi C, Calabrese F, Pettenazzo E, Valente M, Alfieri O, Thiene G & Ferrari R. (2007). Relevance of apoptosis in influencing recovery of hibernating myocardium. *Eur J Heart Fail* **9,** 377-383.

Anghelina M, Krishnan P, Moldovan L & Moldovan NI. (2006). Monocytes/macrophages cooperate with progenitor cells during neovascularization and tissue repair: conversion of cell columns into fibrovascular bundles. *Am J Pathol* **168,** 529-541.

Asahara T, Murohara T, Sullivan A, Silver M, van der Zee R, Li T, Witzenbichler B, Schatteman G & Isner JM. (1997). Isolation of putative progenitor endothelial cells for angiogenesis. *Science* **275,** 964-967.

Askari AT, Unzek S, Popovic ZB, Goldman CK, Forudi F, Kiedrowski M, Rovner A, Ellis SG, Thomas JD, DiCorleto PE, Topol EJ & Penn MS. (2003). Effect of stromal-cell-derived factor 1 on stem-cell homing and tissue regeneration in ischaemic cardiomyopathy. *Lancet* **362,** 697-703.

Balsam LB, Wagers AJ, Christensen JL, Kofidis T, Weissman IL & Robbins RC. (2004). Haematopoietic stem cells adopt mature haematopoietic fates in ischaemic myocardium. *Nature* **428,** 668-673.

Bartunek J, Sherman W, Vanderheyden M, Fernandez-Aviles F, Wijns W & Terzic A. (2009). Delivery of biologics in cardiovascular regenerative medicine. *Clin Pharmacol Ther* **85,** 548-552.

Bax JJ, Schinkel AF, Boersma E, Elhendy A, Rizzello V, Maat A, Roelandt JR, van der Wall EE & Poldermans D. (2004). Extensive left ventricular remodeling does not allow viable myocardium to improve in left ventricular ejection fraction after revascularization and is associated with worse long-term prognosis. *Circulation* **110,** II18-22.

Beanlands RS, Hendry PJ, Masters RG, deKemp RA, Woodend K & Ruddy TD. (1998). Delay in revascularization is associated with increased mortality rate in patients with severe left ventricular dysfunction and viable myocardium on fluorine 18-fluorodeoxyglucose positron emission tomography imaging. *Circulation* **98,** II51-56.

Beanlands RS, Ruddy TD, deKemp RA, Iwanochko RM, Coates G, Freeman M, Nahmias C, Hendry P, Burns RJ, Lamy A, Mickleborough L, Kostuk W, Fallen E & Nichol G. (2002). Positron emission tomography and recovery following revascularization (PARR-1): the importance of scar and the development of a prediction rule for the degree of recovery of left ventricular function. *J Am Coll Cardiol* **40,** 1735-1743.

Bearzi C, Rota M, Hosoda T, Tillmanns J, Nascimbene A, De Angelis A, Yasuzawa-Amano S, Trofimova I, Siggins RW, Lecapitaine N, Cascapera S, Beltrami AP, D'Alessandro DA, Zias E, Quaini F, Urbanek K, Michler RE, Bolli R, Kajstura J, Leri A & Anversa P. (2007). Human cardiac stem cells. *Proc Natl Acad Sci U S A* **104,** 14068-14073.

Beltrami AP, Barlucchi L, Torella D, Baker M, Limana F, Chimenti S, Kasahara H, Rota M, Musso E, Urbanek K, Leri A, Kajstura J, Nadal-Ginard B & Anversa P. (2003). Adult cardiac stem cells are multipotent and support myocardial regeneration. *Cell* **114,** 763-776.

Beltrami AP, Urbanek K, Kajstura J, Yan SM, Finato N, Bussani R, Nadal-Ginard B, Silvestri F, Leri A, Beltrami CA & Anversa P. (2001). Evidence that human cardiac myocytes divide after myocardial infarction. *N Engl J Med* **344,** 1750-1757.

Bengel FM, Higuchi T, Javadi MS & Lautamaki R. (2009). Cardiac positron emission tomography. *J Am Coll Cardiol* **54,** 1-15.

Besancon MF, Kyles AE, Griffey SM & Gregory CR. (2004). Evaluation of the characteristics of venous occlusion after placement of an ameroid constrictor in dogs. *Vet Surg* **33,** 597-605.

BioPAL. General Protocol For Blood Flow Experiments
, ed. BioPAL.

Boccafoschi F, Habermehl J, Vesentini S & Mantovani D. (2005). Biological performances of collagen-based scaffolds for vascular tissue engineering. *Biomaterials* **26,** 7410-7417.

Boodhwani M, Mieno S, Feng J, Sodha NR, Clements RT, Xu SH & Sellke FW. (2008a). Atorvastatin impairs the myocardial angiogenic response to chronic ischemia in normocholesterolemic swine. *J Thorac Cardiovasc Surg* **135,** 117-122.

Boodhwani M, Nakai Y, Mieno S, Voisine P, Bianchi C, Araujo EG, Feng J, Michael K, Li J & Sellke FW. (2006). Hypercholesterolemia impairs the myocardial angiogenic response in a swine model of chronic ischemia: role of endostatin and oxidative stress. *Ann Thorac Surg* **81,** 634-641.

Boodhwani M, Voisine P, Ruel M, Sodha NR, Feng J, Xu SH, Bianchi C & Sellke FW. (2008b). Comparison of vascular endothelial growth factor and fibroblast growth factor-2 in a swine model of endothelial dysfunction. *Eur J Cardiothorac Surg* **33,** 645-650; discussion 251-642.

Borgers M & Ausma J. (1995). Structural aspects of the chronic hibernating myocardium in man. *Basic Res Cardiol* **90,** 44-46.

Borgers M, ThonÈ F, Wouters L, Ausma J, Shivalkar B & Flameng W. (1993). Structural correlates of regional myocardial dysfunction in patients with critical coronary artery stenosis: Chronic hibernation? *Cardiovascular Pathology* **2,** 237-245.

Bree D, Wollmuth JR, Cupps BP, Krock MD, Howells A, Rogers J, Moazami N & Pasque MK. (2006). Low-dose dobutamine tissue-tagged magnetic resonance imaging with 3-dimensional strain analysis allows assessment of myocardial viability in patients with ischemic cardiomyopathy. *Circulation* **114,** I33-36.

Buckberg GD, Luck JC, Payne DB, Hoffman JI, Archie JP & Fixler DE. (1971). Some sources of error in measuring regional blood flow with radioactive microspheres. *J Appl Physiol* **31,** 598-604.

Burwash IG, Lortie M, Pibarot P, de Kemp RA, Graf S, Mundigler G, Khorsand A, Blais C, Baumgartner H, Dumesnil JG, Hachicha Z, DaSilva J & Beanlands RS. (2008). Myocardial blood flow in patients with low-flow, low-gradient aortic stenosis: differences between true and pseudo-severe aortic stenosis. Results from the

multicentre TOPAS (Truly or Pseudo-Severe Aortic Stenosis) study. *Heart* **94,** 1627-1633.

Caillaud D, Calderon J, Reant P, Lafitte S, Dos Santos P, Couffinhal T, Roques X & Barandon L. (2010). Echocardiographic analysis with a two-dimensional strain of chronic myocardial ischemia induced with ameroid constrictor in the pig. *Interact Cardiovasc Thorac Surg*.

Camici P, Ferrannini E & Opie LH. (1989). Myocardial metabolism in ischemic heart disease: basic principles and application to imaging by positron emission tomography. *Prog Cardiovasc Dis* **32,** 217-238.

Camici PG & Dutka DP. (2001). Repetitive stunning, hibernation, and heart failure: contribution of PET to establishing a link. *Am J Physiol Heart Circ Physiol* **280,** H929-936.

Camici PG, Prasad SK & Rimoldi OE. (2008). Stunning, hibernation, and assessment of myocardial viability. *Circulation* **117,** 103-114.

Canty JM, Jr. & Fallavollita JA. (2000). Chronic hibernation and chronic stunning: a continuum. *J Nucl Cardiol* **7,** 509-527.

Cerqueira MD, Weissman NJ, Dilsizian V, Jacobs AK, Kaul S, Laskey WK, Pennell DJ, Rumberger JA, Ryan T & Verani MS. (2002). Standardized myocardial segmentation and nomenclature for tomographic imaging of the heart. A statement for healthcare professionals from the Cardiac Imaging Committee of the Council on Clinical Cardiology of the American Heart Association. *Int J Cardiovasc Imaging* **18,** 539-542.

Chen SL, Zhu CC, Liu YQ, Tang LJ, Yi L, Yu BJ & Wang DJ. (2009a). Mesenchymal stem cells genetically modified with the angiopoietin-1 gene enhanced arteriogenesis in a porcine model of chronic myocardial ischaemia. *J Int Med Res* **37,** 68-78.

Chen SY, Wang F, Yan XY, Zhou Q, Ling Q, Ling JX, Rong YZ & Li YG. (2009b). Autologous transplantation of EPCs encoding FGF1 gene promotes neovascularization in a porcine model of chronic myocardial ischemia. *Int J Cardiol* **135,** 223-232.

Cho HJ, Lee N, Lee JY, Choi YJ, Ii M, Wecker A, Jeong JO, Curry C, Qin G & Yoon YS. (2007). Role of host tissues for sustained humoral effects after endothelial progenitor cell transplantation into the ischemic heart. *J Exp Med* **204,** 3257-3269.

Conway EM, Collen D & Carmeliet P. (2001). Molecular mechanisms of blood vessel growth. *Cardiovasc Res* **49,** 507-521.

Dai T, Zheng H & Fu GS. (2008). Hypoxia confers protection against apoptosis via the PI3K/Akt pathway in endothelial progenitor cells. *Acta Pharmacol Sin* **29,** 1425-1431.

Dai W, Hale SL, Kay GL, Jyrala AJ & Kloner RA. (2009). Delivering stem cells to the heart in a collagen matrix reduces relocation of cells to other organs as assessed by nanoparticle technology. *Regen Med* **4,** 387-395.

de Mel A, Jell G, Stevens MM & Seifalian AM. (2008). Biofunctionalization of biomaterials for accelerated in situ endothelialization: a review. *Biomacromolecules* **9,** 2969-2979.

DeGrado TR, Hanson MW, Turkington TG, Delong DM, Brezinski DA, Vallee JP, Hedlund LW, Zhang J, Cobb F, Sullivan MJ & Coleman RE. (1996). Estimation of myocardial blood flow for longitudinal studies with 13N-labeled ammonia and positron emission tomography. *J Nucl Cardiol* **3,** 494-507.

Demirkol MO. (2008). Myocardial viability testing in patients with severe left ventricular dysfunction by SPECT and PET. *Anadolu Kardiyol Derg* **8 Suppl 2,** 60-70.

Depre C & Vatner SF. (2007). Cardioprotection in stunned and hibernating myocardium. *Heart Fail Rev* **12,** 307-317.

Dilsizian V, Bacharach SL, Beanlands RS, Bergmann SR, Delbeke D, Gropler RJ, Knuuti J, Schelbert HR & Travin MI. (2009). PET myocardial perfusion and metabolism clinical imaging. *J Nucl Cardiol* **16,** 651.

Dzau VJ, Braun-Dullaeus RC & Sedding DG. (2002). Vascular proliferation and atherosclerosis: new perspectives and therapeutic strategies. *Nat Med* **8,** 1249-1256.

Elsässer A & Schaper J. (1995). Hibernating myocardium: adaptation or degeneration? *Basic Res Cardiol* **90,** 47-48.

Erbs S, Linke A, Adams V, Lenk K, Thiele H, Diederich KW, Emmrich F, Kluge R, Kendziorra K, Sabri O, Schuler G & Hambrecht R. (2005). Transplantation of blood-derived progenitor cells after recanalization of chronic coronary artery occlusion: first randomized and placebo-controlled study. *Circ Res* **97,** 756-762.

Fallavollita JA. (2000). Spatial heterogeneity in fasting and insulin-stimulated (18)F-2-deoxyglucose uptake in pigs with hibernating myocardium. *Circulation* **102,** 908-914.

Fallavollita JA, Logue M & Canty JM, Jr. (2001). Stability of hibernating myocardium in pigs with a chronic left anterior descending coronary artery stenosis: absence of

progressive fibrosis in the setting of stable reductions in flow, function and coronary flow reserve. *J Am Coll Cardiol* **37,** 1989-1995.

Fedak PW, Szmitko PE, Weisel RD, Altamentova SM, Nili N, Ohno N, Verma S, Fazel S, Strauss BH & Li RK. (2005). Cell transplantation preserves matrix homeostasis: a novel paracrine mechanism. *J Thorac Cardiovasc Surg* **130,** 1430-1439.

Formigli L, Perna AM, Meacci E, Cinci L, Margheri M, Nistri S, Tani A, Silvertown J, Orlandini G, Porciani C, Zecchi-Orlandini S, Medin J & Bani D. (2007). Paracrine effects of transplanted myoblasts and relaxin on post-infarction heart remodelling. *J Cell Mol Med* **11,** 1087-1100.

Fowler JS & Ido T. (2002). Initial and subsequent approach for the synthesis of 18FDG. *Semin Nucl Med* **32,** 6-12.

Freedman SB & Isner JM. (2002). Therapeutic angiogenesis for coronary artery disease. *Ann Intern Med* **136,** 54-71.

Fuchs S, Hendel RC, Baim DS, Moses JW, Pierre A, Laham RJ, Hong MK, Kuntz RE, Pietrusewicz M, Bonow RO, Mintz GS, Leon MB & Kornowski R. (2001). Comparison of endocardial electromechanical mapping with radionuclide perfusion imaging to assess myocardial viability and severity of myocardial ischemia in angina pectoris. *Am J Cardiol* **87,** 874-880.

Fuchs S & Kornowski R. (2005). Correlation between endocardial voltage mapping and myocardial perfusion: implications for the assessment of myocardial ischemia. *Coron Artery Dis* **16,** 163-167.

Gale NW & Yancopoulos GD. (1999). Growth factors acting via endothelial cell-specific receptor tyrosine kinases: VEGFs, angiopoietins, and ephrins in vascular development. *Genes Dev* **13,** 1055-1066.

Gerber BL, Ordoubadi FF, Wijns W, Vanoverschelde JL, Knuuti MJ, Janier M, Melon P, Blanksma PK, Bol A, Bax JJ, Melin JA & Camici PG. (2001). Positron emission tomography using(18)F-fluoro-deoxyglucose and euglycaemic hyperinsulinaemic glucose clamp: optimal criteria for the prediction of recovery of post-ischaemic left ventricular dysfunction. Results from the European Community Concerted Action Multicenter study on use of(18)F-fluoro-deoxyglucose Positron Emission Tomography for the Detection of Myocardial Viability. *Eur Heart J* **22,** 1691-1701.

Gnecchi M, He H, Noiseux N, Liang OD, Zhang L, Morello F, Mu H, Melo LG, Pratt RE, Ingwall JS & Dzau VJ. (2006). Evidence supporting paracrine hypothesis for Akt-modified mesenchymal stem cell-mediated cardiac protection and functional improvement. *FASEB J* **20,** 661-669.

Gonzales C & Pedrazzini T. (2009). Progenitor cell therapy for heart disease. *Exp Cell Res* **315,** 3077-3085.

Gyongyosi M, Sochor H, Khorsand A, Gepstein L & Glogar D. (2001). Online myocardial viability assessment in the catheterization laboratory via NOGA electroanatomic mapping: Quantitative comparison with thallium-201 uptake. *Circulation* **104,** 1005-1011.

Hearse DJ. (2000). The elusive coypu: the importance of collateral flow and the search for an
alternative to the dog. *Cardiovasc Res* **45,** 215-219.

Hein S & Schaper J. (2001). The extracellular matrix in normal and diseased myocardium. *J Nucl Cardiol* **8,** 188-196.

Heymann MA, Payne BD, Hoffman JI & Rudolph AM. (1977). Blood flow measurements with radionuclide-labeled particles. *Prog Cardiovasc Dis* **20,** 55-79.

Heyndrickx GR, Millard RW, McRitchie RJ, Maroko PR & Vatner SF. (1975). Regional myocardial functional and electrophysiological alterations after brief coronary artery occlusion in conscious dogs. *J Clin Invest* **56,** 978-985.

Hill JM, Zalos G, Halcox JP, Schenke WH, Waclawiw MA, Quyyumi AA & Finkel T. (2003). Circulating endothelial progenitor cells, vascular function, and cardiovascular risk. *N Engl J Med* **348,** 593-600.

Hirschi KK, Ingram DA & Yoder MC. (2008). Assessing identity, phenotype, and fate of endothelial progenitor cells. *Arterioscler Thromb Vasc Biol* **28,** 1584-1595.

Hoffmann R, Altiok E, Nowak B, Kuhl H, Kaiser HJ, Buell U & Hanrath P. (2005). Strain rate analysis allows detection of differences in diastolic function between viable and nonviable myocardial segments. *J Am Soc Echocardiogr* **18,** 330-335.

Hou D, Youssef EA, Brinton TJ, Zhang P, Rogers P, Price ET, Yeung AC, Johnstone BH, Yock PG & March KL. (2005). Radiolabeled cell distribution after intramyocardial, intracoronary, and interstitial retrograde coronary venous delivery: implications for current clinical trials. *Circulation* **112,** I150-156.

Hu Q, Suzuki G, Young RF, Page BJ, Fallavollita JA & Canty JM, Jr. (2009). Reductions in mitochondrial O(2) consumption and preservation of high-energy phosphate levels after simulated ischemia in chronic hibernating myocardium. *Am J Physiol Heart Circ Physiol* **297,** H223-232.

Huang NF, Yu J, Sievers R, Li S & Lee RJ. (2005). Injectable biopolymers enhance angiogenesis after myocardial infarction. *Tissue Eng* **11,** 1860-1866.

Hughes GC, Biswas SS, Yin B, Coleman RE, DeGrado TR, Landolfo CK, Lowe JE, Annex BH & Landolfo KP. (2004). Therapeutic angiogenesis in chronically ischemic porcine myocardium: comparative effects of bFGF and VEGF. *Ann Thorac Surg* **77,** 812-818.

Hughes GC, Landolfo CK, Yin B, DeGrado TR, Coleman RE, Landolfo KP & Lowe JE. (2001). Is chronically dysfunctional yet viable myocardium distal to a severe coronary stenosis hypoperfused? *Ann Thorac Surg* **72,** 163-168.

Hughes GC, Post MJ, Simons M & Annex BH. (2003). Translational physiology: porcine models of human coronary artery disease: implications for preclinical trials of therapeutic angiogenesis. *J Appl Physiol* **94,** 1689-1701.

Hur J, Yoon CH, Lee CS, Kim TY, Oh IY, Park KW, Kim JH, Lee HS, Kang HJ, Chae IH, Oh BH, Park YB & Kim HS. (2007). Akt is a key modulator of endothelial progenitor cell trafficking in ischemic muscle. *Stem Cells* **25,** 1769-1778.

Husmann L, Herzog BA, Pazhenkottil AP, Buechel RR, Nkoulou R, Ghadri JR, Valenta I, Burger IA, Gaemperli O, Wyss CA & Kaufmann PA. (2011). Lowering heart rate with an optimised breathing protocol for prospectively ECG-triggered CT coronary angiography. *Br J Radiol* **84,** 790-795.

Ibrahim T, Nekolla SG, Hornke M, Bulow HP, Dirschinger J, Schomig A & Schwaiger M. (2005). Quantitative measurement of infarct size by contrast-enhanced magnetic resonance imaging early after acute myocardial infarction: comparison with single-photon emission tomography using Tc99m-sestamibi. *J Am Coll Cardiol* **45,** 544-552.

Ii M, Nishimura H, Iwakura A, Wecker A, Eaton E, Asahara T & Losordo DW. (2005). Endothelial progenitor cells are rapidly recruited to myocardium and mediate protective effect of ischemic preconditioning via "imported" nitric oxide synthase activity. *Circulation* **111,** 1114-1120.

Ikonen TS, Patila T, Virtanen K, Lommi J, Lappalainen K, Kankuri E, Krogerus L & Harjula A. (2007). Ligation of ameroid-stenosed coronary artery leads to reproducible myocardial infarction--a pilot study in a porcine model. *J Surg Res* **142,** 195-201.

Iozzo P, Chareonthaitawee P, Dutka D, Betteridge DJ, Ferrannini E & Camici PG. (2002). Independent association of type 2 diabetes and coronary artery disease with myocardial insulin resistance. *Diabetes* **51,** 3020-3024.

Jackson KA, Majka SM, Wang H, Pocius J, Hartley CJ, Majesky MW, Entman ML, Michael LH, Hirschi KK & Goodell MA. (2001). Regeneration of ischemic cardiac muscle and vascular endothelium by adult stem cells. *J Clin Invest* **107,** 1395-1402.

Jawad H, Lyon AR, Harding SE, Ali NN & Boccaccini AR. (2008). Myocardial tissue engineering. *Br Med Bull* **87,** 31-47.

Johnson LL, Schofield L, Donahay T, Bouchard M, Poppas A & Haubner R. (2008). Radiolabeled arginine-glycine-aspartic acid peptides to image angiogenesis in swine model of hibernating myocardium. *JACC Cardiovasc Imaging* **1,** 500-510.

Judd RM, Wagner A, Rehwald WG, Albert T & Kim RJ. (2005). Technology insight: assessment of myocardial viability by delayed-enhancement magnetic resonance imaging. *Nat Clin Pract Cardiovasc Med* **2,** 150-158.

Kalka C, Masuda H, Takahashi T, Kalka-Moll WM, Silver M, Kearney M, Li T, Isner JM & Asahara T. (2000). Transplantation of ex vivo expanded endothelial progenitor cells for therapeutic neovascularization. *Proc Natl Acad Sci U S A* **97,** 3422-3427.

Kamihata H, Matsubara H, Nishiue T, Fujiyama S, Amano K, Iba O, Imada T & Iwasaka T. (2002). Improvement of collateral perfusion and regional function by implantation of peripheral blood mononuclear cells into ischemic hibernating myocardium. *Arterioscler Thromb Vasc Biol* **22,** 1804-1810.

Kamihata H, Matsubara H, Nishiue T, Fujiyama S, Tsutsumi Y, Ozono R, Masaki H, Mori Y, Iba O, Tateishi E, Kosaki A, Shintani S, Murohara T, Imaizumi T & Iwasaka T. (2001). Implantation of bone marrow mononuclear cells into ischemic myocardium enhances collateral perfusion and regional function via side supply of angioblasts, angiogenic ligands, and cytokines. *Circulation* **104,** 1046-1052.

Karatzis EN. (2005). The role of inflammatory agents in endothelial function and their contribution to atherosclerosis. *Hellenic J Cardiol* **46,** 232-239.

Kawamoto A, Gwon HC, Iwaguro H, Yamaguchi JI, Uchida S, Masuda H, Silver M, Ma H, Kearney M, Isner JM & Asahara T. (2001). Therapeutic potential of ex vivo expanded endothelial progenitor cells for myocardial ischemia. *Circulation* **103,** 634-637.

Kawamoto A, Tkebuchava T, Yamaguchi J, Nishimura H, Yoon YS, Milliken C, Uchida S, Masuo O, Iwaguro H, Ma H, Hanley A, Silver M, Kearney M, Losordo DW, Isner JM & Asahara T. (2003). Intramyocardial transplantation of autologous endothelial progenitor cells for therapeutic neovascularization of myocardial ischemia. *Circulation* **107,** 461-468.

Keck A, Hertting K, Schwartz Y, Kitzing R, Weber M, Leisner B, Franke C, Bahlmann E, Schneider C, Twisselmann T, Weisbach M, Kuchler R & Kuck KH. (2002). Electromechanical mapping for determination of myocardial contractility and viability. A comparison with echocardiography, myocardial single-photon emission computed tomography, and positron emission tomography. *J Am Coll Cardiol* **40,** 1067-1074; discussion 1075-1068.

Kemp BJ, Kim C, Williams JJ, Ganin A & Lowe VJ. (2006). NEMA NU 2-2001 performance measurements of an LYSO-based PET/CT system in 2D and 3D acquisition modes. *J Nucl Med* **47,** 1960-1967.

Khorsand A, Graf S, Pirich C, Muzik O, Kletter K, Dudczak R, Maurer G, Sochor H, Schuster E & Porenta G. (2005). Assessment of myocardial perfusion by dynamic N-13 ammonia PET imaging: comparison of 2 tracer kinetic models. *J Nucl Cardiol* **12,** 410-417.

Kim HA, Rhim T & Lee M. (2011). Regulatory systems for hypoxia-inducible gene expression in ischemic heart disease gene therapy. *Adv Drug Deliv Rev*.

Klein R, Beanlands RS & deKemp RA. (2010a). Quantification of myocardial blood flow and flow reserve: Technical aspects. *J Nucl Cardiol* **17,** 555-570.

Klein R, Renaud JM, Ziadi MC, Thorn SL, Adler A, Beanlands RS & deKemp RA. (2010b). Intra- and inter-operator repeatability of myocardial blood flow and myocardial flow reserve measurements using rubidium-82 pet and a highly automated analysis program. *J Nucl Cardiol* **17,** 600-616.

Kocher AA, Schuster MD, Szabolcs MJ, Takuma S, Burkhoff D, Wang J, Homma S, Edwards NM & Itescu S. (2001). Neovascularization of ischemic myocardium by human bone-marrow-derived angioblasts prevents cardiomyocyte apoptosis, reduces remodeling and improves cardiac function. *Nat Med* **7,** 430-436.

Kodama K, Kusuoka H, Sakai A, Adachi T, Hasegawa S, Ueda Y, Mishima M, Hori M, Kamada T, Inoue M & Hirayama A. (1996). Collateral channels that develop after an acute myocardial infarction prevent subsequent left ventricular dilation. *J Am Coll Cardiol* **27,** 1133-1139.

Krause K, Schneider C, Lange C, Kokturk B, Boczor S, Geidel S, Salhi A, Alaser J, Zander AR, Kuck KH & Jaquet K. (2009). Endocardial electrogram analysis after intramyocardial injection of mesenchymal stem cells in the chronic ischemic myocardium. *Pacing Clin Electrophysiol* **32,** 1319-1328.

Krenning G, van Luyn MJ & Harmsen MC. (2009). Endothelial progenitor cell-based neovascularization: implications for therapy. *Trends Mol Med* **15,** 180-189.

Kumar A, Bis KG, Shetty A, Vyas A, Anderson A, Balasubramaniam M, O'Neill W & Stein W. (2007). Aortic root catheter-directed coronary CT angiography in swine: coronary enhancement with minimum volume of iodinated contrast material. *AJR Am J Roentgenol* **188,** W415-422.

Kuraitis D, Hou C, Zhang Y, Vulesevic B, Sofrenovic T, McKee D, Sharif Z, Ruel M & Suuronen EJ. (2011). Ex vivo generation of a highly potent population of circulating angiogenic cells using a collagen matrix. *J Mol Cell Cardiol* **51,** 187-197.

Kuraitis D, Suuronen EJ, Sellke FW & Ruel M. (2010). The future of regenerating the myocardium. *Curr Opin Cardiol* **25,** 575-582.

Kutschka I, Chen IY, Kofidis T, Arai T, von Degenfeld G, Sheikh AY, Hendry SL, Pearl J, Hoyt G, Sista R, Yang PC, Blau HM, Gambhir SS & Robbins RC. (2006). Collagen matrices enhance survival of transplanted cardiomyoblasts and contribute to functional improvement of ischemic rat hearts. *Circulation* **114,** I167-173.

Lai T, Fallon JT, Liu J, Mangion J, Gillam L, Waters D & Chen C. (2000). Reversibility and pathohistological basis of left ventricular remodeling in hibernating myocardium. *Cardiovasc Pathol* **9,** 323-335.

Langer R & Tirrell DA. (2004). Designing materials for biology and medicine. *Nature* **428,** 487-492.

Lev EI, Kleiman NS, Birnbaum Y, Harris D, Korbling M & Estrov Z. (2005). Circulating endothelial progenitor cells and coronary collaterals in patients with non-ST segment elevation myocardial infarction. *J Vasc Res* **42,** 408-414.

Lin Y, Weisdorf DJ, Solovey A & Hebbel RP. (2000). Origins of circulating endothelial cells and endothelial outgrowth from blood. *J Clin Invest* **105,** 71-77.

Litvak J, Siderides LE & Vineberg AM. (1957). The experimental production of coronary artery insufficiency and occlusion. *Am Heart J* **53,** 505-518.

Losordo DW, Schatz RA, White CJ, Udelson JE, Veereshwarayya V, Durgin M, Poh KK, Weinstein R, Kearney M, Chaudhry M, Burg A, Eaton L, Heyd L, Thorne T, Shturman L, Hoffmeister P, Story K, Zak V, Dowling D, Traverse JH, Olson RE, Flanagan J, Sodano D, Murayama T, Kawamoto A, Kusano KF, Wollins J, Welt F, Shah P, Soukas P, Asahara T & Henry TD. (2007). Intramyocardial transplantation of autologous CD34+ stem cells for intractable angina: a phase I/IIa double-blind, randomized controlled trial. *Circulation* **115,** 3165-3172.

Maes AF, Borgers M, Flameng W, Nuyts JL, van de Werf F, Ausma JJ, Sergeant P & Mortelmans LA. (1997). Assessment of myocardial viability in chronic coronary

artery disease using technetium-99m sestamibi SPECT. Correlation with histologic and positron emission tomographic studies and functional follow-up. *J Am Coll Cardiol* **29,** 62-68.

Maisonpierre PC, Suri C, Jones PF, Bartunkova S, Wiegand SJ, Radziejewski C, Compton D, McClain J, Aldrich TH, Papadopoulos N, Daly TJ, Davis S, Sato TN & Yancopoulos GD. (1997). Angiopoietin-2, a natural antagonist for Tie2 that disrupts in vivo angiogenesis. *Science* **277,** 55-60.

Mari C & Strauss WH. (2002). Detection and characterization of hibernating myocardium. *Nucl Med Commun* **23,** 311-322.

Maxwell MP, Hearse DJ & Yellon DM. (1987). Species variation in the coronary collateral circulation during regional myocardial ischaemia: a critical determinant of the rate of evolution and extent of myocardial infarction. *Cardiovasc Res* **21,** 737-746.

McLean DS, Anadiotis AV & Lerakis S. (2009). Role of echocardiography in the assessment of myocardial viability. *Am J Med Sci* **337,** 349-354.

Melero-Martin JM, De Obaldia ME, Kang SY, Khan ZA, Yuan L, Oettgen P & Bischoff J. (2008). Engineering robust and functional vascular networks in vivo with human adult and cord blood-derived progenitor cells. *Circ Res* **103,** 194-202.

Miyamoto Y, Suyama T, Yashita T, Akimaru H & Kurata H. (2007). Bone marrow subpopulations contain distinct types of endothelial progenitor cells and angiogenic cytokine-producing cells. *J Mol Cell Cardiol* **43,** 627-635.

Miyasaka Y, Haiden M, Kamihata H, Nishiue T & Iwasaka T. (2005). Usefulness of strain rate imaging in detecting ischemic myocardium during dobutamine stress. *Int J Cardiol* **102,** 225-231.

Moldovan NI, Goldschmidt-Clermont PJ, Parker-Thornburg J, Shapiro SD & Kolattukudy PE. (2000). Contribution of monocytes/macrophages to compensatory neovascularization: the drilling of metalloelastase-positive tunnels in ischemic myocardium. *Circ Res* **87,** 378-384.

Mukherjee D, Bhatt DL, Roe MT, Patel V & Ellis SG. (1999). Direct myocardial revascularization and angiogenesis--how many patients might be eligible? *Am J Cardiol* **84,** 598-600, A598.

Murry CE, Soonpaa MH, Reinecke H, Nakajima H, Nakajima HO, Rubart M, Pasumarthi KB, Virag JI, Bartelmez SH, Poppa V, Bradford G, Dowell JD, Williams DA & Field LJ. (2004). Haematopoietic stem cells do not transdifferentiate into cardiac myocytes in myocardial infarcts. *Nature* **428,** 664-668.

Ninomiya M, Koyama H, Miyata T, Hamada H, Miyatake S, Shigematsu H & Takamoto S. (2003). Ex vivo gene transfer of basic fibroblast growth factor improves cardiac function and blood flow in a swine chronic myocardial ischemia model. *Gene Ther* **10,** 1152-1160.

Nitzsche EU, Choi Y, Czernin J, Hoh CK, Huang SC & Schelbert HR. (1996). Noninvasive quantification of myocardial blood flow in humans. A direct comparison of the [13N]ammonia and the [15O]water techniques. *Circulation* **93,** 2000-2006.

O'Konski MS, White FC, Longhurst J, Roth D & Bloor CM. (1987). Ameroid constriction of the proximal left circumflex coronary artery in swine. A model of limited coronary collateral circulation. *Am J Cardiovasc Pathol* **1,** 69-77.

Page B, Young R, Iyer V, Suzuki G, Lis M, Korotchkina L, Patel MS, Blumenthal KM, Fallavollita JA & Canty JM, Jr. (2008). Persistent regional downregulation in mitochondrial enzymes and upregulation of stress proteins in swine with chronic hibernating myocardium. *Circ Res* **102,** 103-112.

Parkash R, deKemp RA, Ruddy TD, Kitsikis A, Hart R, Beauchesne L, Williams K, Davies RA, Labinaz M & Beanlands RS. (2004). Potential utility of rubidium 82 PET quantification in patients with 3-vessel coronary artery disease. *J Nucl Cardiol* **11,** 440-449.

Patila T, Ikonen T, Kankuri E, Ahonen A, Krogerus L, Lauerma K & Harjula A. (2009). Spontaneous recovery of myocardial function after ligation of Ameroid-stenosed coronary artery. *Scand Cardiovasc J* **43,** 408-416.

Peichev M, Naiyer AJ, Pereira D, Zhu Z, Lane WJ, Williams M, Oz MC, Hicklin DJ, Witte L, Moore MA & Rafii S. (2000). Expression of VEGFR-2 and AC133 by circulating human CD34(+) cells identifies a population of functional endothelial precursors. *Blood* **95,** 952-958.

Penicka M, Widimsky P, Kobylka P, Kozak T & Lang O. (2005). Images in cardiovascular medicine. Early tissue distribution of bone marrow mononuclear cells after transcoronary transplantation in a patient with acute myocardial infarction. *Circulation* **112,** e63-65.

Penn MS & Mangi AA. (2008). Genetic enhancement of stem cell engraftment, survival, and efficacy. *Circ Res* **102,** 1471-1482.

Pokushalov E, Romanov A, Chernyavsky A, Larionov P, Terekhov I, Artyomenko S, Poveshenko O, Kliver E, Shirokova N, Karaskov A & Dib N. (2010). Efficiency of intramyocardial injections of autologous bone marrow mononuclear cells in patients with ischemic heart failure: a randomized study. *J Cardiovasc Transl Res* **3,** 160-168.

Post MJ, Laham R, Sellke FW & Simons M. (2001). Therapeutic angiogenesis in cardiology using protein formulations. *Cardiovasc Res* **49,** 522-531.

Prater DN, Case J, Ingram DA & Yoder MC. (2007). Working hypothesis to redefine endothelial progenitor cells. *Leukemia* **21,** 1141-1149.

Prinzen FW & Bassingthwaighte JB. (2000). Blood flow distributions by microsphere deposition methods. *Cardiovasc Res* **45,** 13-21.

Radke PW, Heinl-Green A, Frass OM, Post MJ, Sato K, Geddes DM & Alton EW. (2006). Evaluation of the porcine ameroid constrictor model of myocardial ischemia for therapeutic angiogenesis studies. *Endothelium* **13,** 25-33.

Rahimtoola SH. (1985). A perspective on the three large multicenter randomized clinical trials of coronary bypass surgery for chronic stable angina. *Circulation* **72,** V123-135.

Rahimtoola SH, La Canna G & Ferrari R. (2006). Hibernating myocardium: another piece of the puzzle falls into place. *J Am Coll Cardiol* **47,** 978-980.

Rehman J, Li J, Orschell CM & March KL. (2003). Peripheral blood "endothelial progenitor cells" are derived from monocyte/macrophages and secrete angiogenic growth factors. *Circulation* **107,** 1164-1169.

Reinhardt CP, Dalhberg S, Tries MA, Marcel R & Leppo JA. (2001). Stable labeled microspheres to measure perfusion: validation of a neutron activation assay technique. *Am J Physiol Heart Circ Physiol* **280,** H108-116.

Robich MP, Osipov RM, Chu LM, Feng J, Burgess TA, Oyamada S, Clements RT, Laham RJ & Sellke FW. (2010). Temporal and spatial changes in collateral formation and function during chronic myocardial ischemia. *J Am Coll Surg* **211,** 470-480.

Roth DM, Maruoka Y, Rogers J, White FC, Longhurst JC & Bloor CM. (1987). Development of coronary collateral circulation in left circumflex Ameroid-occluded swine myocardium. *Am J Physiol* **253,** H1279-1288.

Roth DM, White FC, Nichols ML, Dobbs SL, Longhurst JC & Bloor CM. (1990). Effect of long-term exercise on regional myocardial function and coronary collateral development after gradual coronary artery occlusion in pigs. *Circulation* **82,** 1778-1789.

Ruel M, Laham RJ, Parker JA, Post MJ, Ware JA, Simons M & Sellke FW. (2002). Long-term effects of surgical angiogenic therapy with fibroblast growth factor 2 protein. *J Thorac Cardiovasc Surg* **124,** 28-34.

Ruel M, Song J & Sellke FW. (2004). Protein-, gene-, and cell-based therapeutic angiogenesis for the treatment of myocardial ischemia. *Mol Cell Biochem* **264,** 119-131.

Ruel M, Wu GF, Khan TA, Voisine P, Bianchi C, Li J, Laham RJ & Sellke FW. (2003a). Inhibition of the cardiac angiogenic response to surgical FGF-2 therapy in a Swine endothelial dysfunction model. *Circulation* **108 Suppl 1,** II335-340.

Ruel MA, Sellke FW, Bianchi C, Khan TA, Faro R, Zhang JP & Cohn WE. (2003b). Endogenous myocardial angiogenesis and revascularization using a gastric submucosal patch. *Ann Thorac Surg* **75,** 1443-1449.

Sato K, Wu T, Laham RJ, Johnson RB, Douglas P, Li J, Sellke FW, Bunting S, Simons M & Post MJ. (2001). Efficacy of intracoronary or intravenous VEGF165 in a pig model of chronic myocardial ischemia. *J Am Coll Cardiol* **37,** 616-623.

Schaper W. (1971). *The Collateral Circulation of the Heart*. American Elsevier Publishing, New York.

Schelbert HR, Beanlands R, Bengel F, Knuuti J, Dicarli M, Machac J & Patterson R. (2003). PET myocardial perfusion and glucose metabolism imaging: Part 2-Guidelines for interpretation and reporting. *J Nucl Cardiol* **10,** 557-571.

Schelbert HR, Phelps ME, Huang SC, MacDonald NS, Hansen H, Selin C & Kuhl DE. (1981). N-13 ammonia as an indicator of myocardial blood flow. *Circulation* **63,** 1259-1272.

Schiller NB, Shah PM, Crawford M, DeMaria A, Devereux R, Feigenbaum H, Gutgesell H, Reichek N, Sahn D, Schnittger I & et al. (1989). Recommendations for quantitation of the left ventricle by two-dimensional echocardiography. American Society of Echocardiography Committee on Standards, Subcommittee on Quantitation of Two-Dimensional Echocardiograms. *J Am Soc Echocardiogr* **2,** 358-367.

Schinkel AF, Bax JJ, Poldermans D, Elhendy A, Ferrari R & Rahimtoola SH. (2007). Hibernating myocardium: diagnosis and patient outcomes. *Curr Probl Cardiol* **32,** 375-410.

Schinkel AF, Poldermans D, Rizzello V, Vanoverschelde JL, Elhendy A, Boersma E, Roelandt JR & Bax JJ. (2004). Why do patients with ischemic cardiomyopathy and a substantial amount of viable myocardium not always recover in function after revascularization? *J Thorac Cardiovasc Surg* **127,** 385-390.

Schneider C, Jaquet K, Geidel S, Rau T, Malisius R, Boczor S, Zienkiewicz T, Kuck KH & Krause K. (2009). Transplantation of bone marrow-derived stem cells improves

myocardial diastolic function: strain rate imaging in a model of hibernating myocardium. *J Am Soc Echocardiogr* **22,** 1180-1189.

Schneider C, Jaquet K, Malisius R, Geidel S, Bahlmann E, Boczor S, Rau T, Antz M, Kuck KH & Krause K. (2007). Attenuation of cardiac remodelling by endocardial injection of erythropoietin: ultrasonic strain-rate imaging in a model of hibernating myocardium. *Eur Heart J* **28,** 499-509.

Schneider C, Krause K, Jaquet K, Geidel S, Malisius R, Boczor S, Rau T, Zienkiewicz T, Hennig D & Kuck KH. (2008). Intramyocardial transplantation of bone marrow-derived stem cells: ultrasonic strain rate imaging in a model of hibernating myocardium. *J Card Fail* **14,** 861-872.

Schuh A, Liehn EA, Sasse A, Hristov M, Sobota R, Kelm M, Merx MW & Weber C. (2008). Transplantation of endothelial progenitor cells improves neovascularization and left ventricular function after myocardial infarction in a rat model. *Basic Res Cardiol* **103,** 69-77.

Schwarz ER, Schoendube FA, Kostin S, Schmiedtke N, Schulz G, Buell U, Messmer BJ, Morrison J, Hanrath P & vom Dahl J. (1998). Prolonged myocardial hibernation exacerbates cardiomyocyte degeneration and impairs recovery of function after revascularization. *J Am Coll Cardiol* **31,** 1018-1026.

Semenza GL. (2007). Vasculogenesis, angiogenesis, and arteriogenesis: mechanisms of blood vessel formation and remodeling. *J Cell Biochem* **102,** 840-847.

Sereda CW & Adin CA. (2005). Methods of gradual vascular occlusion and their applications in treatment of congenital portosystemic shunts in dogs: a review. *Vet Surg* **34,** 83-91.

Shen YT, Kudej RK, Bishop SP & Vatner SF. (1996). Inotropic reserve and histological appearance of hibernating myocardium in conscious pigs with ameroid-induced coronary stenosis. *Basic Res Cardiol* **91,** 479-485.

Shetty AN, Bis KG, Vyas AR, Kumar A, Anderson A & Balasubramaniam M. (2008). Contrast volume reduction with superior vena cava catheter-directed coronary CT angiography: comparison with peripheral i.v. contrast enhancement in a swine model. *AJR Am J Roentgenol* **190,** W247-254.

Silva GV, Fernandes MR, Cardoso CO, Sanz RR, Oliveira EM, Jimenez-Quevedo P, Lopez J, Angeli FS, Zheng Y, Willerson JT & Perin EC. (2011). A dosing study of bone marrow mononuclear cells for transendocardial injection in a pig model of chronic ischemic heart disease. *Tex Heart Inst J* **38,** 219-224.

Silva GV, Litovsky S, Assad JA, Sousa AL, Martin BJ, Vela D, Coulter SC, Lin J, Ober J, Vaughn WK, Branco RV, Oliveira EM, He R, Geng YJ, Willerson JT & Perin

EC. (2005). Mesenchymal stem cells differentiate into an endothelial phenotype, enhance vascular density, and improve heart function in a canine chronic ischemia model. *Circulation* **111,** 150-156.

Smith PK. (2009). Treatment selection for coronary artery disease: The collision of a belief system with evidence. *J Thorac Cardiovasc Surg* **137,** 1050-1053.

Statistic-Canada. Table 102-0529 - Deaths, by cause, Chapter IX: Diseases of the circulatory system (I00 to I99), age group and sex, Canada, annual (number) 2000 to 2006, CANSIM (database). .

Steiner S, Niessner A, Ziegler S, Richter B, Seidinger D, Pleiner J, Penka M, Wolzt M, Huber K, Wojta J, Minar E & Kopp CW. (2005). Endurance training increases the number of endothelial progenitor cells in patients with cardiovascular risk and coronary artery disease. *Atherosclerosis* **181,** 305-310.

Suri C, Jones PF, Patan S, Bartunkova S, Maisonpierre PC, Davis S, Sato TN & Yancopoulos GD. (1996). Requisite role of angiopoietin-1, a ligand for the TIE2 receptor, during embryonic angiogenesis. *Cell* **87,** 1171-1180.

Suuronen EJ, Kuraitis D & Ruel M. (2008). Improving cell engraftment with tissue engineering. *Semin Thorac Cardiovasc Surg* **20,** 110-114.

Suuronen EJ, Muzakare L, Doillon CJ, Kapila V, Li F, Ruel M & Griffith M. (2006a). Promotion of angiogenesis in tissue engineering: developing multicellular matrices with multiple capacities. *Int J Artif Organs* **29,** 1148-1157.

Suuronen EJ, Price J, Veinot JP, Ascah K, Kapila V, Guo XW, Wong S, Mesana TG & Ruel M. (2007). Comparative effects of mesenchymal progenitor cells, endothelial progenitor cells, or their combination on myocardial infarct regeneration and cardiac function. *J Thorac Cardiovasc Surg* **134,** 1249-1258.

Suuronen EJ, Veinot JP, Wong S, Kapila V, Price J, Griffith M, Mesana TG & Ruel M. (2006b). Tissue-engineered injectable collagen-based matrices for improved cell delivery and vascularization of ischemic tissue using CD133+ progenitors expanded from the peripheral blood. *Circulation* **114,** I138-144.

Suuronen EJ, Zhang P, Kuraitis D, Cao X, Melhuish A, McKee D, Li F, Mesana TG, Veinot JP & Ruel M. (2009). An acellular matrix-bound ligand enhances the mobilization, recruitment and therapeutic effects of circulating progenitor cells in a hindlimb ischemia model. *FASEB J* **23,** 1447-1458.

Thurston G, Suri C, Smith K, McClain J, Sato TN, Yancopoulos GD & McDonald DM. (1999). Leakage-resistant blood vessels in mice transgenically overexpressing angiopoietin-1. *Science* **286,** 2511-2514.

Townsend DW. (2004). Physical principles and technology of clinical PET imaging. *Ann Acad Med Singapore* **33,** 133-145.

Townsend DW, Beyer T, Jerin J, Watson CC, Young J & Nutt R. (1999). The ECAT ART Scanner for Positron Emission Tomography. 1. Improvements in Performance Characteristics. *Clinical positron imaging : official journal of the Institute for Clinical PET* **2,** 5-15.

Tse HF, Kwong YL, Chan JK, Lo G, Ho CL & Lau CP. (2003). Angiogenesis in ischaemic myocardium by intramyocardial autologous bone marrow mononuclear cell implantation. *Lancet* **361,** 47-49.

Tse HF, Thambar S, Kwong YL, Rowlings P, Bellamy G, McCrohon J, Thomas P, Bastian B, Chan JK, Lo G, Ho CL, Chan WS, Kwong RY, Parker A, Hauser TH, Chan J, Fong DY & Lau CP. (2007). Prospective randomized trial of direct endomyocardial implantation of bone marrow cells for treatment of severe coronary artery diseases (PROTECT-CAD trial). *Eur Heart J* **28,** 2998-3005.

Tuzun E, Oliveira E, Narin C, Khalil H, Jimenez-Quevedo P, Perin E & Silva G. (2009). Correlation of Ischemic Area and Coronary Flow With Ameroid Size in a Porcine Model. *J Surg Res*.

Uemura R, Xu M, Ahmad N & Ashraf M. (2006). Bone marrow stem cells prevent left ventricular remodeling of ischemic heart through paracrine signaling. *Circ Res* **98,** 1414-1421.

Unger EF. (2001). Experimental evaluation of coronary collateral development. *Cardiovasc Res* **49,** 497-506.

van Ramshorst J, Bax JJ, Beeres SL, Dibbets-Schneider P, Roes SD, Stokkel MP, de Roos A, Fibbe WE, Zwaginga JJ, Boersma E, Schalij MJ & Atsma DE. (2009). Intramyocardial bone marrow cell injection for chronic myocardial ischemia: a randomized controlled trial. *JAMA* **301,** 1997-2004.

Vasa M, Fichtlscherer S, Aicher A, Adler K, Urbich C, Martin H, Zeiher AM & Dimmeler S. (2001). Number and migratory activity of circulating endothelial progenitor cells inversely correlate with risk factors for coronary artery disease. *Circ Res* **89,** E1-7.

Vitale GD, deKemp RA, Ruddy TD, Williams K & Beanlands RS. (2001). Myocardial glucose utilization and optimization of (18)F-FDG PET imaging in patients with non-insulin-dependent diabetes mellitus, coronary artery disease, and left ventricular dysfunction. *J Nucl Med* **42,** 1730-1736.

Vogt AM, Elsasser A, Nef H, Bode C, Kubler W & Schaper J. (2003). Increased glycolysis as protective adaptation of energy depleted, degenerating human hibernating myocardium. *Mol Cell Biochem* **242,** 101-107.

von Ritter C, Hinder RA, Womack W, Bauerfeind P, Fimmel CJ, Kvietys PR, Granger DN & Blum AL. (1988). Microsphere estimates of blood flow: methodological considerations. *Am J Physiol* **254,** G275-279.

Wang X, Hu Q, Nakamura Y, Lee J, Zhang G, From AH & Zhang J. (2006). The role of the sca-1+/CD31- cardiac progenitor cell population in postinfarction left ventricular remodeling. *Stem Cells* **24,** 1779-1788.

Wen Y, Meng L, Xie J & Ouyang J. (2011). Direct autologous bone marrow-derived stem cell transplantation for ischemic heart disease: a meta-analysis. *Expert Opin Biol Ther* **11,** 559-567.

Werner N, Kosiol S, Schiegl T, Ahlers P, Walenta K, Link A, Bohm M & Nickenig G. (2005). Circulating endothelial progenitor cells and cardiovascular outcomes. *N Engl J Med* **353,** 999-1007.

White FC, Carroll SM, Magnet A & Bloor CM. (1992). Coronary collateral development in swine after coronary artery occlusion. *Circ Res* **71,** 1490-1500.

Wu J, Zeng F, Weisel RD & Li RK. (2009). Stem cells for cardiac regeneration by cell therapy and myocardial tissue engineering. *Adv Biochem Eng Biotechnol* **114,** 107-128.

Wu KC & Lima JA. (2003). Noninvasive imaging of myocardial viability: current techniques and future developments. *Circ Res* **93,** 1146-1158.

Yamaguchi J, Kusano KF, Masuo O, Kawamoto A, Silver M, Murasawa S, Bosch-Marce M, Masuda H, Losordo DW, Isner JM & Asahara T. (2003). Stromal cell-derived factor-1 effects on ex vivo expanded endothelial progenitor cell recruitment for ischemic neovascularization. *Circulation* **107,** 1322-1328.

Yoder MC, Mead LE, Prater D, Krier TR, Mroueh KN, Li F, Krasich R, Temm CJ, Prchal JT & Ingram DA. (2007). Redefining endothelial progenitor cells via clonal analysis and hematopoietic stem/progenitor cell principals. *Blood* **109,** 1801-1809.

Zhang Y, Thorn S, DaSilva JN, Lamoureux M, DeKemp RA, Beanlands RS, Ruel M & Suuronen EJ. (2008). Collagen-based matrices improve the delivery of transplanted circulating progenitor cells: development and demonstration by ex vivo radionuclide cell labeling and in vivo tracking with positron-emission tomography. *Circ Cardiovasc Imaging* **1,** 197-204.

Zhu CC, Chen SL, Lin XF, Tang LJ, Gan MF, Zhu GQ, Bao WG, Zhou WJ, Ye ZR, Ye MH & Ma DH. (2008). [Create a standard mini-swine model of chronic ischemic myocardium by thoracoscopy]. *Zhonghua Wai Ke Za Zhi* **46,** 1163-1165.